

Energy & Environmental Science

Accepted Manuscript



This is an *Accepted Manuscript*, which has been through the Royal Society of Chemistry peer review process and has been accepted for publication.

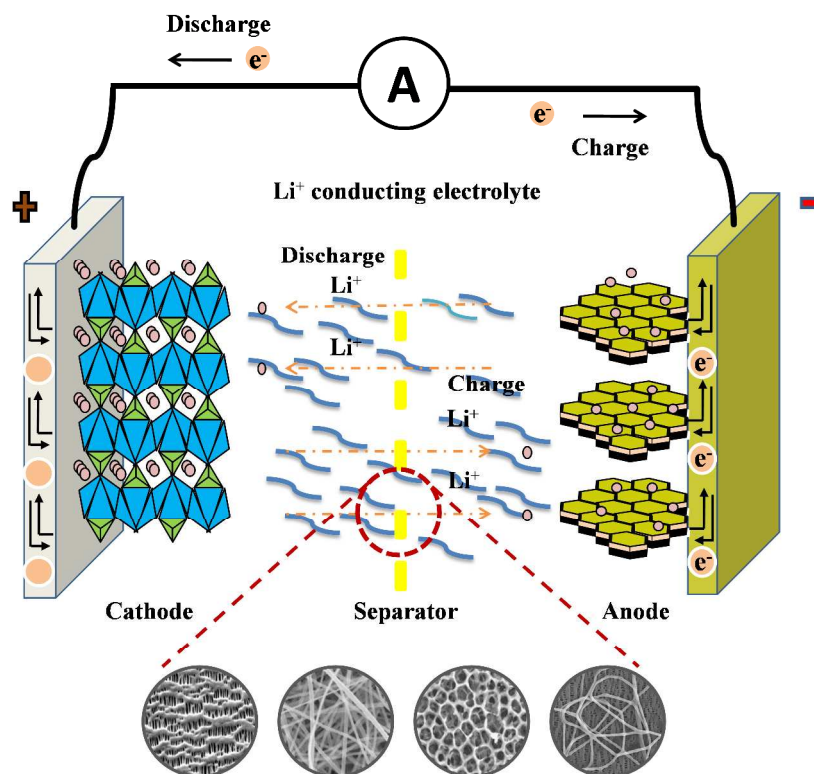
Accepted Manuscripts are published online shortly after acceptance, before technical editing, formatting and proof reading. Using this free service, authors can make their results available to the community, in citable form, before we publish the edited article. We will replace this *Accepted Manuscript* with the edited and formatted *Advance Article* as soon as it is available.

You can find more information about *Accepted Manuscripts* in the [Information for Authors](#).

Please note that technical editing may introduce minor changes to the text and/or graphics, which may alter content. The journal's standard [Terms & Conditions](#) and the [Ethical guidelines](#) still apply. In no event shall the Royal Society of Chemistry be held responsible for any errors or omissions in this *Accepted Manuscript* or any consequences arising from the use of any information it contains.

Table of Contents (TOC) Graphic

The separator of a lithium-ion battery prevents the direct contact between the positive and negative electrodes while serving as the electrolyte reservoir to enable the transportation of lithium ions between the two electrodes.



A Review and Recent Developments in Membrane Separators for Rechargeable Lithium-ion Batteries

Hun Lee, Meltem Yanilmaz, Ozan Toprakci, Kun Fu, and Xiangwu Zhang*

Fiber and Polymer Science Program, Department of Textile Engineering, Chemistry and
Science, North Carolina State University, Raleigh, NC 27695-8301, USA

* Author to whom correspondence should be addressed.

Tel: 919-515-6547; Fax: 919-515-6532; E-mail: xiangwu_zhang@ncsu.edu

Abstract

In this paper, the recent developments and their characteristics of membrane separators for lithium-ion batteries are reviewed. In recent years, there have been intensive efforts to develop advanced battery separators for rechargeable lithium-ion batteries for different applications such as portable electronics, electric vehicles, and energy storage for power grids. Separator is a critical component of lithium-ion batteries since it provides a physical barrier between the positive and negative electrodes in order to prevent electrical short circuits. The separator also serves as the electrolyte reservoir for the transport of ions during the charging and discharging cycles of a battery. The performance of lithium-ion batteries is greatly affected by the materials and structure of the separators. This paper introduces the requirements of battery separators and the structure and properties of five important types of membrane separators which are microporous membranes, modified microporous membranes, non-woven mats, composite membranes and electrolyte membranes. Each separator type has inherent advantages and disadvantages which influence the performance of lithium-ion batteries. The structures, characteristics, manufacturing, modification, and performance of separators are described in this review paper. The outlooks and future directions in this research field are also given.

Keywords: Separator, Membrane, Polyolefin, Lithium-ion battery, Energy storage

Broader Context

In recent years, there have been intensive efforts to develop high-performance battery separators for rechargeable lithium-ion batteries for different applications such as portable electronics, electric vehicles, and energy storage for power grids. Separator is a critical component of lithium-ion batteries since separator prevents physical contact between the positive and negative electrodes of the battery while serving as the electrolyte reservoir to enable ionic transport. The performance of lithium-ion batteries is greatly affected by the materials and structure of the separators. The major goals of this review article are to highlight the recent developments and advances of membrane separators for lithium-ion batteries and to give a broad picture of recent scientific research on separator materials for high-performance lithium-ion batteries.

1. Introduction on lithium-ion battery

Lithium-ion batteries have received considerable attention as the most popular energy storage system for a wide variety of portable electronic devices including laptops, digital cameras, and cell phones with the worldwide market valued at ten billion dollars. They are also one of the most promising candidates as the large-scale power source for electric vehicles and emerging smart grids because they have several important advantages including high energy density, no memory effect, long cycle life, and low self-discharging. Similar to the architecture of basic Galvanic cells, a lithium-ion battery consists of three functional components, *i.e.*, anode (negative electrode), cathode (positive electrode), and electrolyte (Figure 1). When the battery is discharged, lithium ions move from the anode to the cathode through the non-aqueous electrolyte, carrying the current. During charging, an external electrical power source forces the current to pass in the reverse direction and make lithium ions migrate from the cathode to the anode across the electrolyte.

The separator is placed between the anode and the cathode. In a lithium-ion battery, the essential function of the separator is to prevent the physical contact of electrodes while serving as the electrolyte reservoir to enable ionic transport. The separator does not involve directly in any cell reactions, but its structure and properties play an important role in determining the battery performance, including cycle life, safety, energy density, and power density, through influencing the cell kinetics. A wide variety of factors should be considered while selecting appropriate separators for use in lithium-ion batteries. Table 1 summarizes the general requirements that should be considered for lithium-ion battery separators. These requirements are discussed in detail in the following section.

2. Requirements for separators

Separators must be chemically and electrochemically stable to the electrolyte and electrode materials in lithium-ion batteries. They should be inert under the strong oxidizing and reducing conditions when the battery is fully discharged and charged. They should not produce impurities, which can cause interference to the function of the batteries. In some applications, separators have to withstand the corrosive nature of the electrolyte at elevated temperatures.

The wettability by liquid electrolyte is an important property for battery separators since electrolyte absorption is required for ion transport. Separators must absorb and retain a significantly amount of liquid electrolyte to achieve low internal resistance and high ionic conductivity. The fast absorption of liquid electrolyte facilitates the process of electrolyte filling during the battery assembly. The filling speed depends on the type of the materials, porosity, and pore size of the separators.

The mechanical properties of separators are characterized by the tensile strength and puncture strength in the machine direction (MD) and the transverse direction (TD). The separators must be strong enough to withstand the tension of winding operation during battery assembly. For a battery separator with 25 μm in thickness, the minimum tensile strength measured according to ASTM D882 and D638 is 98.06 MPa. Separators should also have high puncture strength to withstand the penetration of electrode materials. If particulate materials from the electrodes pass through the separator, electrical short circuit of the battery

occurs. The puncture strength of the separators for normal lithium-ion battery applications should be at least 300 g/mil using ASTM D3763.

Separators used in rechargeable batteries typically are 20 – 50 μm in thickness, but separators for most commercial lithium-ion batteries are in the range of 20 – 25 μm [1]. Batteries with thin separators often have lower internal resistance, and exhibit high energy and power densities. However, thin separators may have adverse effects on the mechanical strength and safety. On the other hand, thicker separators give greater mechanical strength during cell assembly and lead to improved battery safety. In addition, the uniformity of separator thickness plays a critical role in the stable and long cycle life of the batteries.

The pore size of separators is a key characteristic. The pores should be small enough to block the penetration of particles, including the electrode components such as active materials and conducting additives. Uniform distribution and tortuous structure of the pores contribute to the inhibition of dendritic lithium and prevent particles from penetrating the separators. Typically, submicron pore size (less than 1 μm) is desirable for separators used in lithium-ion batteries.

Separators should have appropriate porosity to retain adequate liquid electrolyte so that the batteries can have sufficient ionic conductivity. If the porosity is too low, the internal resistance will be high because of insufficient liquid electrolyte between the two electrodes. However, if the porosity is too high, it adversely impacts the battery safety because it could cause low mechanical strength. In addition, separators with too high porosities tend to shrink when the temperature increases.

The separator porosity is defined by the ratio of void volume to apparent geometric volume [2], and it can be calculated by the following equation:

$$\text{Porosity (\%)} = \left(1 - \frac{\rho_M}{\rho_P}\right) \times 100 \quad (1)$$

where ρ_M is the apparent density of the separator, and ρ_P the density of the polymer. In practice, the porosity is often measured by the weights of the separator before and after the absorption of a liquid as the following equation:

$$\text{Porosity (\%)} = \frac{W - W_0}{\rho_L V_0} \times 100 \quad (2)$$

where W_0 and W represent the weights of the separator before and after immersing a liquid, respectively, ρ_L the density of the liquid, and V_0 the geometric volume of the separator. In this equation, it is assumed that the volume occupied by the liquid is equal to the porous volume of the separator. The porosity of around 40-60 % is desirable for normal lithium-ion battery separators.

In addition to the actual porosity, the uniformity of porosity across the separator is critically important. Non-uniform porosity leads to non-uniform current density and reduces the battery performance because the active materials contacting the high-porosity regions may have to work harder compared with those contacting the low-porosity regions.

The permeability of separators can be described by the MacMullin number, which is the ratio of the resistance of the separator immersed with liquid electrolyte to the resistance of

the electrolyte alone. The MacMullin number is proportional to air permeability and it is often expressed by the Gurley value [2]. The Gurley value measures the time required for air to pass through unit area of the separator under a fixed pressure [3]. If the porosity and thickness of the separator are fixed, the Gurley value is determined by the tortuosity of the pores. If the Gurley value is low, the separator has high porosity and low tortuosity. In addition, the uniform permeability of a separator is critical for achieving long cycle life because non-uniform permeability leads to uneven distribution of current density and the dendritic formation on the electrodes. Typically, Gurley values for lithium-ion battery separators are less than $0.025 \text{ sec}/\mu\text{m}$ measured by ASTM D726 and D737.

Separators should be flat and not curl up when they are laid out and immersed with liquid electrolyte. The bow and skew of the separators can cause misalignment while being assembled with the electrodes during the manufacturing of batteries. In addition, separators must not shrink during the storage and operation of batteries.

Separators must not shrink and wrinkle apparently when the temperature rises. The thermal shrinkage during the drying process for battery assembly should be minimized. The requirement of thermal shrinkage is generally less than 5% after 60 min at $90 \text{ }^\circ\text{C}$ [6].

The ability to shut the batteries down when overheating or short circuit occurs is a desirable safety function of separators. The shutdown function should not be achieved by sacrificing the mechanical integrity, which could cause the direct contact of electrodes. Some separators can close the pores and block ionic flows when the thermal runaway temperature is reached. These separators typically have a multilayer design, in which at least one layer melts to close the pores near the thermal runaway temperature and the other layers provide

mechanical strength. When these separators are used, the electrode reactions can be stopped in the batteries before an explosion occurs. Currently, the thermal runaway temperature of these separators is typically 130 °C, which is close to the melting temperature of polyethylene, the polymer used as the functional layer in these separators [6].

Most separators are not ionically conductive and ion transport occurs only after they are filled with liquid electrolyte. The ionic conductivities in the range of 10^{-3} S/cm to 10^{-1} S/cm at room temperature are acceptable in batteries for applications such as microelectronics, medical implants, military industry, automobile, etc [4]. Typically, a conductivity of 10^{-3} S/cm is sufficient in low-power applications such as cell phones. In high-power automobile applications, higher conductivities may be needed. Besides ionic conductivity, electrolyte retention is also critical for long-term use. Although there is no literature report on how high the electrolyte retention should be, it has been well established that low electrolyte retention causes high resistance and leads to poor cycling performance [5].

3. Structure and properties of separators

Battery separators can be divided into five major types: microporous membranes, modified microporous membranes, non-woven mats, composite membranes, and electrolyte membranes depending on their composition and structure. Microporous membrane separators are characterized by pore sizes in the range of micrometers. They can be classified into monolayer and multilayer microporous membranes, depending on the number of layers. Modified microporous membrane separators are the membranes modified from conventional microporous membranes via surface modification like grafting methods using plasma and

irradiation or coating with a different polymer. Non-woven mat separators have web structures bonded together with entangling fibers prepared by melt blown, wet laid, and electrospinning techniques. Since they have small fiber diameters, the non-woven mat separators show higher porosities than other types of separators. Composite membrane separators are prepared by coating or filling inorganic materials to microporous membranes or non-woven mats. Thus, they have outstanding thermal stability and exceptional wettability that other types cannot achieve. Electrolyte membranes include solid ceramic electrolyte, solid polymer electrolyte, gel polymer electrolyte and composite electrolyte. They work as both separator and electrolyte, and offer high battery safety. Each separator type respectively possesses intrinsic features to satisfy the requirements discussed in the previous section, including thickness, porosity, thermal property, wettability, mechanical, and chemical properties.

3.1. Microporous membrane separators

3.1.1. Fabrication processes

Most microporous membrane separators are made of polyethylene (PE), polypropylene (PP), and their combinations such as PE/PP and PP/PE/PP. However, other polymers such as isotactic poly(4-methyl-1-pentene) [7], polyoxymethylene [8,9], PE-PP blend [10-12], polystyrene (PS)-PP blend [13], and poly(ethylene terephthalate (PET)-PP blend polymers [13] have also been used for preparing microporous membranes.

Bierenbaum et al. [14] reviewed the process, physical and chemical properties, and the application of microporous polymer membranes as battery separators. Microporous

membranes can be prepared mainly by two different manufacturing methods: wet process and dry process. Both manufacturing methods basically involve an extrusion step to prepare polymer thin film and a stretching step to form porous structure. Microporous membranes made by dry process have slit-like pores in shape, while those from wet process show interconnected and elliptical pores. Figure 2 compares the microstructures of microporous membranes made by dry process and wet process. The membranes formed by the dry process are more appropriate for high power density batteries because of their open and straight porous structure. On the other hand, the membranes made by the wet process are more suitable in long cycle life batteries because interconnected pores and tortuous structure are beneficial in preventing the growth of dendrites during charging and discharging.

The dry process [7–11,13,15–27] generally consists of heating, extruding, annealing, and stretching steps. Figure 3a shows the main steps of the dry process. After the heating step, the resultant polymer melt is extruded to form a polymer film, which has a nonporous structure with lamellae arranged in the row direction. The annealing step is applied to improve the crystalline structure of the polymer film, thus facilitating the formation of porous structure in the stretching step. The annealed film is then stretched along the machine direction to form micropores. Figure 4 shows the microstructure of a polymer film before and after stretching. Before the stretching step, the polymer film shows a stacked lamellar morphology oriented along the transverse direction (Figure 4a). After stretching, the stacked lamellae are apart from each other and form pores oriented in machine direction (Figure 4b).

The stretching step in the dry process is composed of cold stretch, hot stretch, and relaxation, which is necessary for reducing the internal stresses induced by heat treatment.

The porosity of the resultant membrane depends on the morphology of extruded film, and the conditions of annealing and stretching steps, including annealing temperature, annealing time, stretching ratio, etc. There are uniaxial [7–9] and biaxial stretches [10,22,29] adopted in the industry, but the uniaxial stretching method has been more successful to date. The tensile strength of membranes made by uniaxial stretching is anisotropic in machine and transverse directions mainly because the pore shape is oriented in the machine direction. A higher tensile strength in machine direction than transverse direction is desirable for handling the separators during battery assembly. The dry process is technologically convenient since no solvents are used during the process. Celgard LLC [30–33] and Ube Industries [34] provide PP and PE microporous membrane separators produced by dry process.

The wet process employs the principle of solvent extraction [12,14,29,35–40]. This process generally includes four steps as shown in Figure 3b. The first step is the mixing and heating of polymer, hydrocarbon liquid, and other additives to form a homogenous solution. The second step is to extrude the solution into a nonporous film. The third step is to extract the liquid and other additives by a volatile solvent to form the microporous structure. The fourth step, the stretching of the film, can be conducted before or after the extraction of liquid and additives to achieve desirable porosity and pore size. For the wet process, the microstructure and properties of the resultant microporous membranes depend on the composition of the solutions and the extraction of the solvents as well as annealing and stretching conditions. Figure 5 shows the SEM images of microporous membrane separators prepared by wet process. These microporous membranes exhibit distinct differences in the orientation of pores, pore size, and pore shape.

In addition to conventional dry and wet processes, phase inversion is another extensively studied method for making microporous membrane separators. The phase inversion method also involves the dissolution of a polymer in a good solvent and the precipitation of the polymer to form the microporous structure by solvent exchange [42–45]. When the phase inversion method is used, an asymmetrical porous structure is often formed, with a highly porous morphology on the top, but a less porous, compact structure on the bottom, as shown in Figure 6. The asymmetrical structure of membranes prepared by the phase inversion process is affected by the polymer type and concentration, additive type and concentration, solvent type, membrane thickness, and processing temperature and time. In practical applications, the asymmetrical structure often limits the battery performance because the compact structure on the bottom surface could reduce the absorption of liquid electrolyte and hinders ionic flows. On the bottom side, the substrate often blocks the exchange between the solvent and non-solvent and leads to the formation of a less porous structure. As a result, nonuniform separator structure causes significant deviations in resistance and hinders the ionic flow, which could be a concern especially for large-scale cell operations [3,47-49].

3.1.2. Monolayer membranes

The simplest microporous membrane separator type is monolayer membranes. Monolayer membranes can be made from different polymer materials. Table 2 shows the structural characteristics and properties of various monolayer membranes, including materials, processing methods, electrolyte uptakes, ionic conductivities, and electrochemical performance.

Polyolefins have been widely used as the material for monolayer membrane separators due to their excellent mechanical strength and good chemical stability. Djian et al. [50] evaluated the performance of commercial membrane separators. The membrane separators with higher pore volume and larger pore diameter showed increased conductivity after absorbing the liquid electrolyte. The membrane morphology had no significant effect on the battery performance at low C-rate, but the charge capacities at high C-rate increased when membrane separators with higher porosity and pore size were used.

The porosity, pore size, gas permeability, and thermal properties of commercial PP and PE membrane separators were studied by Venugopal et al. [51]. The relatively low porosity and pore size allowed the membranes to prevent internal shorts between the electrodes and reduce gas permeability. Wu et al. [52] discussed the safety issue of PP and PE membranes. The membranes were evaluated by soft-nail penetration test after charge-discharge cycles. The PP membranes failed in the penetration safety test and the batteries using PP membranes exploded after 200 cycles. On the other hand, the PE membranes had a low shutdown temperature of 130 °C and survived in the safety test.

Love [53] studied the mechanical and thermal properties of commercial PP and PE membranes. The PP membranes by dry process showed anisotropic structure and weak tensile strength in the transverse direction. On the other hand, the PE membranes by wet process had a biaxial structure and nearly identical strength on both directions. The author observed losses in mechanical strength of the membranes exposed to the various temperatures and after immersing them in an electrolyte solution.

Ihm et al. [54] investigated the effect of polymer blending and stretching conditions on the mechanical properties of PE microporous membrane separators. The mechanical strength increased with increase in the molecular weight of high-density polyethylene (HDPE) and the content of ultra-high molecular weight polyethylene (UHMWPE). The membranes made by stretching after extraction showed larger pore size and wider distribution of pore size than those prepared by stretching before the extraction step.

Although polyolefin microporous monolayer membranes are the most commonly used in lithium-ion batteries, their intrinsic characteristics such as poor thermal stability, low wettability and poor electrolyte retention properties restrict the realization of high battery performance. To overcome these drawbacks, a variety of polymers have been used for preparing microporous membranes and the three most reported ones are poly(vinylidene fluoride) (PVDF) [55–62], polyacrylonitrile (PAN) [63–67], and poly(methyl methacrylate) (PMMA) [67–70].

Microporous PVDF membranes are physicochemically and electrochemically stable in lithium-ion batteries [55–61]. PVDF membranes are mechanically strong and have great wettability due to good affinity of PVDF to liquid electrolyte solutions. Magistris et al. [58] investigated the microstructure of PVDF membranes prepared by a phase inversion method. The morphologies of membranes were divided into sponge-like and finger-like structures. They claimed that the electrolyte solution was not only contained in the porous structure, but also formed swollen gel phases with PVDF, which increased the ionic conductivity. However, when PVDF membranes are used, LiF could be formed because of the interaction between lithium ions and the fluorine atoms in PVDF.

Microporous PAN membranes have also been developed for use as separators in lithium-ion batteries [63,66,67]. They exhibit good processability, high thermal stability, desirable morphology for high electrolyte uptake, excellent electrochemical stability, and good compatibility with electrodes. In addition, PAN can act as a polymer matrix to help maintain liquid electrolyte and participate in lithium ion transport due to the interaction between the lithium ion and the $C\equiv N$ groups of PAN. PAN membranes can also minimize the formation of dendrites during the charging/discharging process of lithium-ion batteries. As a result, PAN membranes show high ionic conductivity and good electrochemical stability in lithium-ion batteries. However, PAN membranes often suffer from electrolyte leakage during long-term storage [71].

Like PVDF and PAN, PMMA is also used for making microporous membrane separators [67–70] because it has high affinity to the liquid electrolyte. PMMA membranes were studied in terms of the mechanism of membrane formation, chemical structure, hydrophilicity, morphology, thermodynamic properties, and polymer-solvent compatibility. Those membranes show high equivalent conductivity and good thermal and electrochemical stabilities. PMMA membranes also exhibit high ionic conductivity and good adhesion to the electrodes because of the formation of gel phases with liquid electrolyte. However, PMMA has poor mechanical strength due to its amorphous structure [72].

The high crystallinity of microporous monolayer membranes is one of major causes for the relatively high internal resistance of some lithium-ion batteries. Since the crystalline region of the polymer membranes hinders the migration of lithium ions, batteries with those membranes often exhibit low charge/discharge capacity and poor C-rate value [3,6,64,69,73].

In order to reduce the crystallinity and improve the ionic conductivity, many copolymers have been utilized as materials for microporous membrane separators, including poly(vinylidene fluoride-co-hexafluoropropylene) (PVDF-co-HFP) [73–75], poly(hydroxyethyl acrylate-co-acrylonitrile) (PHEA-co-AN) [76], poly(methyl methacrylate-acrylonitrile-vinyl acetate) (PMMA-AN-VAc) [77], and polyacrylonitrile-methyl methacrylate) (PAN-MMA) [78]. Among all these copolymers, PVDF-co-HFP has drawn the most attention as a separator material for lithium-ion batteries because it has high affinity to liquid electrolyte solution, good electrochemical stability, and desirable adhesion with the electrodes. The amorphous HFP phase helps capture a large amount of liquid electrolyte while the PVDF crystalline phase acts as a mechanical support for the polymer membrane. PVDF-co-HFP also has high dielectric constant and electron withdrawing fluorine atoms in the polymer backbone. This feature is advantageous to dissociate the lithium salt to lithium ions. Highly porous PVDF-co-HFP membranes were prepared by using phase inversion method and their microstructure and performance were reported by Shi et al. [74]. The processing conditions such as temperature and solution composition determined the porous structure of the membranes, including porosity and pore size. Small pores with narrow pore size distribution were beneficial in maintaining the liquid electrolyte and high porosity led to high conductivity.

Microporous monolayer membranes made by polymer blends have been also prepared in order to improve the ionic conductivity by decreasing the crystalline regions. These membranes can combine advantages offered by both polymers, including mechanical properties, thermal stability, wettability, and electrochemical stability. Subramania et al. [79]

prepared microporous membranes by phase inversion using PVDF-co-HFP and PAN blends. It was observed that the ionic conductivity of microporous membranes increased with increase in PAN content. These blend membranes had thermal stability up to 161 °C and offered higher battery capacity than membranes based on PAN or PVDF alone. Jung et al.[80] prepared microporous PAN/poly(vinylpyrrolidone) (PVP) blend membranes by the phase inversion method. The asymmetric structure of the membranes on the through-thickness direction became more obvious when the molecular weight of PVP was high. The permeability of membranes increased as the PVP content decreased.

PVDF/PMMA blends [81,82, 83] and polyvinylchloride (PVC)/PMMA blend [84] were also used for preparing microporous membranes. The microporous structure was formed by casting the polymer blend solution and extracting additives. The mechanical properties were stable in temperatures ranging from 20 °C to 140 °C. The amorphous phase of the membranes increased with increasing PMMA content, which helped the formation of polymer gel phases. When the PMMA content was 60% in the blend, the membrane showed the most favorable ionic conductivity and lithium self-diffusion after absorbing liquid electrolyte. The ionic conductivity of liquid electrolyte-soaked membranes increased with increasing PMMA content because of the good affinity of PMMA to liquid electrolyte.

Poly(acrylonitrile-co-butyl acrylate) (PAN-co-BuA)/PVC blends were used for the preparation of microporous membranes by phase inversion [85]. The mechanical strength of the blend membranes was found to be much higher than that of pure PAN-co-BuA ones, depending on the blend composition. These blend membranes exhibited ionic conductivity of higher than 1.5×10^{-3} S/cm and electrochemical stability of up to 4.8 V after absorbing the

liquid electrolyte. The good overall properties of these blend membranes were attributed to PAN-co-BuA acting as a conducting channel and PVC providing the mechanical strength.

Microporous membranes based on PVDF-co-HFP and cyanoethylated cellulose derivative (DH-4-CN) blends were obtained and characterized by Ren et al. [86]. The tensile strength and thermal property were improved with increase in DH-4-CN content. The ionic conductivity showed a maximum value when the PVDF-co-HFP:DH-4-CN ratio was 14:1, at which the membrane presented the most desirable pore structure. The blends of PVDF-co-HFP/poly(methyl methacrylate-co-acrylonitrile-co-lithium methacrylate) (PMAML) [87], PVDF-co-HFP/poly(ethylene oxide-co-ethylene carbonate) (PEO-co-EC) [88] and PVDF-co-HFP/poly(vinyl acetate) (PVAc) [89], PVDF-TRFE/PEO [90], PVDF/P(MMA-co-PEGMA) [91], PVDF/PDMS-grafted-(PPO-PEO) [92] were also made into microporous membranes. These membranes showed high ionic conductivity and good electrochemical performance because of the improved microstructure through polymer blending. PVDF-TRFE membranes were also evaluated and it was found that the performance of these membranes varied with the processing techniques used [93].

Compared with the multilayer membranes discussed in the following section, monolayer membranes can be prepared using simple methods, leading to relatively low cost. As a result, monolayer membranes have been widely used as lithium-ion battery separators in a wide range of applications.

3.1.3. Multilayer membranes

Microporous monolayer membranes have difficulty to simultaneously attain optimal properties in mechanical strength, thermal resistance, and electrochemical performance. To overcome this drawback, microporous multilayer membrane separators prepared from different polymers have been studied extensively. Microporous multilayer membranes can be prepared by using different methods, including dip coating [94–98], laminating [99–101], slot die [102,103], gravure [104,105], casting [106], phase inversion [107], and so forth. Table 3 summarizes the properties and performance of some multilayer membranes.

Microporous membranes consisting of multilayers of PP and PE have been designed as thermal shutdown separators with a safety advantage. Many patents for PE-PP bilayer [108] and PP-PE-PP trilayer [109,110] membranes have been reported by separator manufacturers. In a multilayer structure, the PE layer melts and blocks the pathway of ions when the temperature is close to the melting temperature of PE. At the same time, the PP layer still remains their dimensional structure and mechanical strength, preventing the short circuit between two electrodes. Hence, such a multilayer structure can provide the safety assurance while maintaining sufficient mechanical strength. The shutdown characteristics of commercial trilayer membranes are often studied by measuring the impedance of batteries as a function of temperature. In addition to the shutdown function, it was also reported that multilayer membranes of PE and PP have higher puncture strength than the corresponding PE or PP monolayer membranes.

Non-woven mats have also been used as the substrate to produce microporous multilayer membranes. Lee et al. [111] described a continuous process to make microporous multilayer membranes by coating non-woven mats. Figure 7 showed the schematic description of the

process that consisted of 4 steps: coating, forming, washing, and winding. The coating solution was prepared by dissolving polymer in a solvent and then coated onto the non-woven substrate. PE non-woven mats are the most used non-woven substrate and they are often made into microporous multilayer membranes by coating acrylonitrile (AN)-methyl methacrylate (MMA) copolymer [112], or PVDF/PVAc blend [113]. The PE non-woven mat provides good mechanical strength and a thermal shut-down property, while the polymer coating layer enhances the compatibility with the liquid electrolyte, leading to good ionic conductivity and electrochemical performance. In addition to PE non-woven mats, poly(ethylene terephthalate) (PET) non-woven mats have also been coated by PVDF [114] and PVDF-co-HFP [115] to make microporous multilayer membranes. The resultant membranes showed high wettability, high ionic conductivity, good mechanical stability, and excellent electrochemical stability.

Cross-linked structures have been created for microporous multilayer membranes with enhanced thermal stabilities. For example, polyethylene glycol dimethacrylate (PEGDMA)/PVDF-co-HFP blend [116,117], polyethylene glycol diacrylate (PEGDA)/PVDF/PMMA blend [118], PEGDA/poly(ethylene glycol) methyl ether acrylate (PEGMEA) blend [119] were used with irradiation method to form chemically cross-linked structures. During the preparation of these membranes, microporous polyolefin membranes were dipped in the blend solutions to form the multilayer membranes with porous coating layers. The coated membranes were then irradiated for cross-linking. The thermal stability of the resultant membranes increased with increasing irradiation dose and cross-linker content. It was also found that the crystallinity decreased as irradiation dose increased and cross-

linker content decreased. High ionic conductivities in order of 10^{-4} S/cm were obtained after immersing these cross-linked multilayer membranes in liquid electrolytes.

Electroactive polymers have been used as coating layers to make microporous multilayer membranes that can effectively shut down the batteries during overcharging. Electroactive polymers are often obtained from the polymerization of conductive monomers, and examples of such polymers are poly(3-butylthiophene) (P3BT) [120], poly(3-Decylthiophene) (P3DT) [121], and poly(triphenylamine) (PTPAn) [122]. Microporous multilayer membranes with appropriate electroactive polymer coatings can transform from conductive state to insulating state at overcharged voltage, effectively protecting the batteries from voltage runaway. The membranes work reversibly and have no significant impact on charge-discharge cycling at normal conditions.

Multilayer membranes with other unique structures have also been prepared. For example, Huai et al. [123] and Park et al. [124] prepared multilayer membranes that have the unique porous structure of PAN and PMMA nanoparticle coatings. During the preparation of these membranes, colloidal solutions of polymer nanoparticles were obtained by conventional emulsion polymerization and applied on the surface of polyolefin non-woven fabrics. Figure 8 shows the microstructures of PAN and PMMA nanoparticle-coated membranes. The polymer nanoparticles formed close-packed coating layers on the polyolefin non-woven fabric surface, forming unique porous structure. These membranes showed good wettability and exhibited high ionic conductivity in the order of 10^{-4} S/cm after absorbing a liquid electrolyte of 1M LiPF₆ in EC/DC/EMC (1:1:1 by weight) or 1M LiPF₆ in EC/DEC (1:1 by volume).

Lee et al. and M. Alcoutlabi prepared microporous multilayer membranes by coating PP microporous membranes with PVDF and PVDF copolymer nanofiber coating layers using the electrospinning method [125,126]. The adhesion properties of the membrane separators onto the positive electrodes were significantly improved by the nanofiber coatings. The nanofiber-coated membranes also showed higher electrolyte uptake than uncoated membranes due to high absorption ability of the electrospun nanofiber coatings.

Taskier et al. [98] prepared hydrophilic microporous membranes by coating a surfactant consisting of silicon glycol copolymers on a hydrophobic PP membrane to increase the wettability and electrolyte retention. However, the surfactant was unstable on the membrane surface. Zhang et al. [127] prepared multilayer membranes by coating PVDF on both sides of a PMMA substrate. The PVDF outer layers were porous and the PMMA inner layer was solid.

Microporous multilayer membranes combine the advantages of each component layers and can address the issues raised from the drawbacks of monolayer membranes. Several microporous multilayer membranes, such as Celgard[®] trilayer separators, have been used in commercial lithium-ion batteries. However, current microporous multilayer membranes can still be improved in terms of thickness, wettability, and ionic conductivity.

3.2. Modified microporous membrane separators

Currently, the most widely used separators in lithium-ion batteries are made of polyolefins, specifically microporous PE and PP membrane separators. However, these membrane separators provide relatively low thermal stability, poor wettability, and

unsatisfactory electrolyte retention. To improve these properties, various methods could be used to modify the structure of microporous polyolefin membrane separators [128–133]. Table 4 shows the properties of modified microporous membrane separators.

One simple and effective method to modify the structure and properties of microporous polyolefin membranes is to graft hydrophilic monomers onto the membrane surfaces. There are various techniques to graft hydrophilic monomers, including plasma, ultraviolet (UV) irradiation, and electron beam irradiation. For example, Kim et al. [134] fabricated modified PE membranes by grafting acrylonitrile (AN) monomers using plasma treatment. The grafting of plasma-induced AN monomers led to a hydrophilic surface and improved the electrolyte wettability and retention.

Electron beam irradiation is another commonly used method to modify the surface hydrophilicity of microporous polyolefin membranes. Gineste et al. [135] modified microporous PP membranes and created hydrophilic surface by grafting acrylic acid and diethylene glycol-dimethacrylate (DEGDM) monomers using electron beam. The modified membranes showed improved electrolyte uptake, ionic conductivity, and cycle life as compared with unmodified PP membranes. Glycidyl methacrylate (GMA) [136] and methyl methacrylate (MMA) [137] have also been grafted onto the surface of PE membranes by using electron beam irradiation. The grafted monomers on the surface of PE membranes increased the electrolyte uptake and retention, leading to improved electrochemical performance. Lee et al. utilized electron beam irradiation to modify PE membranes by grafting poly(ethylene glycol) borate acrylate (PEGBA) [138] and 2,4,6,8-tetramethyl-2,4,6,8-tetravinylcyclotetrasiloxane (Siloxane) [139]. It was found that the degree of grafting

increased and the porosity of modified membranes decreased as the irradiation dose increased. The ionic conductivity of the modified membranes exhibited a magnitude of 10^{-4} S/cm at 10 kGy irradiation dose. Graphite/LiCoO₂ cells using the modified membranes showed improved cycling performance at various current rates, especially at high voltage operating conditions.

Kim et al. [140] investigated the effect of gamma irradiation on the morphological, thermal, and electrochemical properties of PE membranes. The modified membranes experienced morphological changes caused by the crosslinking of PE polymer chains under irradiation. The porosity and pore size of the membranes decreased with increasing irradiation dose. In addition, the modified membranes showed enhanced thermal stability compared to non-irradiated membranes. Graphite/LiCoO₂ cells using modified membranes also exhibited higher discharge capacities than those using unmodified membranes, especially at high rates.

Although most work focuses on modifying the structure and properties of microporous polyolefin membranes, efforts have been taken on the modification of microporous membranes made of other polymers. For example, Gamma and UV irradiations were used to modify PVDF [141,142] and PVDF-co-HFP [143] membranes. These modified membranes showed improved mechanical and electrochemical properties compared to unmodified membranes.

Besides the abovementioned grafting techniques, coating microporous membrane separators using a different polymer is another important approach to modify microporous membrane separators. For example, Lee et al. [144] introduced polydopamine (PDA) surface coating onto PE separators to modify their surface properties in terms of wettability,

electrolyte uptake and thermal stability. Although the porosity and Gurley number of the separators were not affected by PDA coating, the contact angle decreased significantly and ionic conductivity increased as well. In addition, the cells assembled by using PDA-coated separators showed enhanced cycle life and improved C-rate performance due to the combined effect of hydrophilic surfaces, increased liquid electrolyte uptake, inhibited Li-dendrite growth, and improved Catecholic adhesion between Li-metal electrodes and separators [145]. In another study, it was demonstrated that the PDA coating process could enhance the electrolyte wetting, electrolyte uptake, and ionic conductivity, leading to improved C-rate performance and power performance [146]. Fang et al. [147] used polyethylene glycol chains combined with PDA coating to modify PP separators and achieved increased electrolyte uptake, reduced interfacial resistance and enhanced cycling stability. Kang et al. [148] introduced a novel bio-inspired approach to improve the power density and safety of lithium-ion batteries by using PDA coating and subsequent silica coating, which increased the electrolyte wettability of PE membrane separators. In addition to PDA, other materials have been used to coat microporous membrane separators. For example, Li et al. [149] prepared PEO-coated polypropylene separators. Improved ionic conductivity and electrolyte retention were reported due to the swollen PEO gel phase. Shi et al. [150] immobilized PMMA layer onto PE membrane separators by using dopamine treatment and graft polymerization of MMA monomer. The resultant separators exhibited improved electrolyte uptake and ionic conductivity, resulting in higher C-rate and better cycling performance. Song et al. [49] dip coated polyimide to PE separators and increased the thermal stability without diminishing their electrochemical performance. Sohn et al. [151]

reported PVDF-HFP/PMMA-coated PE separators and investigated the effect of coating composition on the morphology and performance of the coated separators. The highest electrolyte uptake, ionic conductivity and cycling performance were obtained by using 5/5 PVDF-HFP/PMMA coated PE separators.

In summary, the modification of microporous membrane separators has led to improvements in mechanical properties, wettability, and ionic conductivity. In addition, the electrochemical performance, especially high-rate capability, of lithium-ion batteries can also be improved by using modified microporous membrane separators.

3.3. Non-woven mat separators

Non-woven mat separators have fibrous structures that gain their structural integrity and strength by entangled fibers. Non-woven mats are typically made by bonding randomly oriented fibers through chemical and mechanical methods. Non-woven mats are traditionally prepared by dry process such as melt-blown method [152–157] and wet process such as wet laid method [158–162] and papermaking method [163,164]. The melt-blown method is a binderless process which can be divided into two steps: forming a fibrous web and bonding the fibrous web. First, melted polymer is extruded through a spinneret or die having holes to form a polymer web consisting of numerous fibers. The fibers are stretched and cooled by high-velocity hot air. In the second step, the resultant web is collected into rolls and subsequently bonded by calendaring at high temperature and pressure to form the non-woven mat with sufficient mechanical strength. On the other hand, the wet process uses a resin as an adhesive. A fibrous web is formed by numerous fibers and the resin is sprayed onto the web

to bond the base fibers with heat and pressure. For both dry and wet processes, the structure and properties of the final non-woven mats depend on various parameters such as polymer type, polymer composition, temperature, and pressure. Non-woven mats prepared by traditional dry and wet processes are often used as separators for lead acid batteries. In general, these nonwoven mats have relatively large fiber diameter and pore size, which are inappropriate for use in lithium-ion batteries.

In order to reduce fiber diameter and pore size, the electrospinning method has been adopted to produce the highly porous non-woven mat separators that are suitable for lithium-ion batteries. Electrospinning is fundamentally different from other mechanically-driven spinning techniques. A typical electrospinning set-up consists of a high voltage power supply, a syringe, a spinning nozzle, and a grounded collector, as shown Figure 9. A high voltage is applied between the electrospinning solution contained in the syringe and the grounded metallic collector. When the voltage reached a critical value, the electrostatic force overcomes the surface tension of the pendant drop of the polymer solution at the tip of the nozzle and a liquid jet is ejected. Nanofibers deposit on the grounded collector and form a non-woven structure. The electrospinning method is known to be a simple and efficient technique for preparing non-woven mats consisting of fibers with diameters in the range of several micrometers down to tens of nanometers. Electrospun non-woven mats have many advantages as battery separators, including high porosity, small pore size, interconnected open pore structure, high permeability, and large surface area. Table 5 summarizes the properties of non-woven mat separators prepared by electrospinning method.

Many polymers can be used to produce electrospun non-woven mats. Among them, PVDF is an excellent material candidate for non-woven mat separators for lithium-ion batteries because it has good electrochemical stability and excellent affinity for lithium ions. Kim et al. [165] prepared and characterized electrospun PVDF non-woven mats as lithium-ion battery separator. The PVDF non-woven mats showed high electrolyte uptake because of the high porosity with large surface area and the swelling ability of PVDF fibers. Figure 10 compares the morphologies of electrospun PVDF non-woven mats before and after absorbing liquid electrolyte. It is seen that fibers were swollen and exhibited increased fiber diameters after absorbing the electrolyte. The ionic conductivities were found to increase with decrease in the average fiber diameter of dried fibers. The authors claimed that the interaction between the high crystalline PVDF fibers and the liquid electrolyte had a minimal effect on the lithium ion transfer because liquid electrolyte hardly passed through the crystalline region of the fibers. Choi et al. [166] also prepared electrospun PVDF non-woven mats and investigated their physical and electrochemical properties. After immersing in a liquid electrolyte, the non-woven mats were partially swollen, but still maintained the structure integrity and exhibited good mechanical strength because of three-dimensional network structure formed by fully-interconnected fibers. The electrochemical properties of the non-woven mats mainly depended on the liquid electrolyte phase held in the porous structure and the gel phase formed by the swelling of electrospun fibers.

The morphology and crystal structure of electrospun PVDF non-woven mats were investigated by Gao et al. [167] to understand the physical properties. The electrospun PVDF non-woven mats exhibited weakened crystallinity but highly oriented molecular chains, which

resulted in improved mechanical properties. The tensile strength of the non-woven mats increased with decrease in fiber diameter because fibers with smaller diameters were prepared under higher applied voltages and had higher draw ratios. The high porosity and uniform pore distribution of electrospun non-woven mats with smaller diameters were also found to be able to suppress the growth of lithium dendrites mechanically, and hence Li/LiMn₂O₄ cells using these non-woven mats as the separator exhibited good cycling behavior.

Choi et al. [168] applied a thermal treatment step on electrospun PVDF non-woven mats to enhance their physical properties and dimensional stability. The mechanical strength of the non-woven mats was improved since the thermal treatment promoted the crystallinity. In addition, after absorbing liquid electrolyte, the thermally-treated PVDF non-woven mats exhibited high ionic conductivities of $1.6 \times 10^{-3} - 2.0 \times 10^{-3}$ S/cm. Lee et al. [169] prepared electrospun PVDF non-woven mats and employed the hot pressing method to reduce the deformation in porous structure in the mats, especially at high charge-discharge rates. They hot-pressed the electrospun PVDF non-woven mats directly between the anode and the cathode. It was found that the resultant Li/LiCoO₂ cells have lower capacities due to the reduced mat porosity and electrolyte uptake. However, the hot-pressed PVDF non-woven mats formed homogeneous gel membranes, leading to good cycle life.

The pore structure and electrochemical performance of PVDF non-woven mats were controlled by spinning conditions, sheet forming process, and post-treatments. Nanofiber membranes with appropriate pore structures showed good C-rate performance with high electrolyte uptake and good mechanical strength [170]. Cao et al. [171] prepared electrospun

PVDF non-woven membranes and they modified these PVDF membranes by using PDA coating. Improved cycling performance and power capability were obtained on cells using PDA-coated PVDF non-woven separators. The improvement in cycling stability and rate capability was explained by the higher uptake capacity, enhanced ionic conductivity, and the Catechol adhesion between the separator and electrode [171]. Liang et al. [172] introduced heat-treated PVDF non-woven membranes with improved strength and good electrochemical performance in terms of electrochemical stability, interfacial resistance and cycling performance. To control the non-woven mat structure, modified electrospinning set-up has also been used to prepare PVDF non-woven mats. For example, spherical hat [173] and rotational [168] drum were used to replace the conventional flat collector during the collection of nanofibers. The resultant PVDF non-woven mats showed higher porosity and better uniformity, thereby leading to increased mechanical strength and improved discharge capacity.

As discussed above, PVDF is the most commonly studied polymer for preparing non-woven mats for use as lithium-ion battery separators. However, PVDF has relatively high crystallinity, and many researchers believe the high crystallinity could cause low ionic conductivity and low stability due to the reduced migration rate of lithium ions in the crystalline phase. One of effective methods for lowering the crystallinity of non-woven mats is to use suitable PVDF copolymers or modified PVDF. For example, electrospun PVDF-co-HFP non-woven mats were prepared and their physical and electrochemical properties were investigated [5,174,175]. Results showed that PVDF-co-HFP non-woven mats had excellent electrochemical properties because the electrolyte uptake was increased due to the good

affinity of PVDF-co-HFP to liquid electrolyte. Figure 11 shows the swelling behavior of electrospun PVDF-co-HFP non-woven mats by absorbing liquid electrolyte. Similar to PVDF nanofibers, the average diameter of PVDF-co-HFP nanofibers increased greatly in liquid electrolyte. The amorphous swollen phase on the surface of electrospun PVDF-co-HFP nanofibers can easily uptake liquid electrolyte and prevent its leakage, while the solid phase in the core of PVDF-co-HFP fibers provides the mechanical support. Li/LiFePO₄ [174,175] cells and mesocarbon microbead (MCMB)/LiCoO₂ [5] cells using these non-woven mat separators exhibited stable charge/discharge properties with little capacity fading.

Kader et al. [176] suggested poly(vinylidene fluoride)-graft-poly(tert-butyl acrylate) (PVDF-g-tBA) membranes fabricated by electrospinning. The degree of crystallinity for PVDF-g-tBA membranes was lower than that of PVDF membranes. Therefore, PVDF-g-tBA based electrospun membranes exhibited higher ionic conductivity, better electrochemical stability, and improved cycling performance. In another study, PVDF-HFP- PTFE composite separator was designed by casting PVDF-HFP on PTFE matrix. Thus, PVDF-HFP can absorb large amount of liquid electrolyte while PTFE matrix improve the mechanical strength [177].

PAN is another polymer that is commonly used in the preparation of electrospun non-woven mats for use as lithium-ion battery separators [178–182] since it has superior characteristics in terms of good mechanical stability and fast lithium ion transport. Electrospun PAN non-woven mats achieve high mechanical strength mainly through the strong interaction of adjacent nitrile (C≡N) groups in PAN polymer chains. Since highly polar nitrile groups hinder the arrangement of polymer chains during electrospinning, flexible

non-woven mats of highly amorphous PAN nanofibers can be prepared with high mechanical strength and large porosity. Electrospun PAN non-woven mats showed high electrolyte uptake and high ionic conductivity because of the highly porous structure and polymer gel phase formed in the amorphous region. Furthermore, the interaction between the nitrile groups in PAN and lithium ions in the electrolyte contributed to high ionic conductivity. The superior cycle performance and rate capability of cells using PAN non-woven mats were also observed. The main reason was believed to be the excellent retention of liquid electrolyte. In addition, it was found that electrospun PAN non-woven mats were able to maintain their porous structure after prolonged charge-discharge cycles, as shown in Figure 12.

In order to improve the affinity to liquid electrolyte and other physical properties, polymer blends have been employed to prepared non-woven mats for use as lithium-ion battery separators. Rao et al. [183] made electrospun PAN/PMMA non-woven mats and compared their properties with those of electrospun PAN non-woven mats. With the same electrospinning conditions, PAN/PMMA non-woven mats showed smaller fiber diameters than PAN non-woven mats, leading to higher porosity. In addition, the PMMA component in electrospun PAN/PMMA non-woven mats had good compatibility with the liquid electrolyte and was able to absorb a large amount of liquid electrolyte. These effects resulted in large electrolyte uptake and high ionic conductivity, 3.6×10^{-3} S/cm. Consequently, Li/LiFePO₄ cells using electrospun PAN/PMMA non-woven mats showed improved cycling and rate performance. Electrospun non-woven mats were also prepared by using polymer blends, such as polyimide (PI)/PVDF [184], PI/PAN [184], PVDF/PAN [71] and PVDF-co-HFP/PMMA [185]. The crystallinity degrees of these mats were depressed due to the blending of two

different polymers. These non-woven mats also possessed improved mechanical properties, large electrolyte uptake, high ionic conductivity, and good electrochemical properties.

The abovementioned electrospun non-woven mats have monolayer structure. Recently, electrospun multilayer non-woven mats have also been prepared. For example, Raghavan et al. [186] developed trilayer non-woven mat separators consisting PAN nanofibers and PVDF-co-HFP nanofibers via electrospinning. Figure 13 shows the schematic of the structure of the trilayer non-woven mat separators. The trilayer separators exhibited high electrolyte uptake and good ionic conductivity in the range of 10^{-3} S/cm. Li/LiFePO₄ cells assembled with trilayer non-woven mat separators showed high electrochemical stability and good cycling performance with slow capacity fading.

In recent years, besides commonly-used separator materials such as PVDF, PAN and PMMA, new polymers such as polyimide, nylon, polysulfonamide, polyethylene terephthalate, etc., have been utilized to prepare separator membranes with improved thermal stability. Jiang et al. [187] reported polyimide-based non-woven membranes by using electrospinning, followed by subsequent thermal imidization and mechanical pressing. Superior electrochemical performance was reported at room temperature and 120 °C due to the high thermal stability of polyimide and the highly porous structure of the non-woven membranes [187]. Other non-woven mat separators with improved thermal stability include, but are not limited to polysulfonamide [188], polyester [189,190], polyphthalazinone ether sulfone ketone (PPESK) [191], PPESK/PVDF/PPESK [192], cellulose/PVDF-HFP [193], cellulose/polysulfonamide [194], and cellulose/PDA based non-woven membranes [195].

These membranes not only showed high thermal stability but also exhibited good electrochemical performance.

As discussed above, most electrospun non-woven mats have desirable structure and properties for use as lithium-ion battery separators. However, compared with microporous membranes and modified microporous membranes, electrospun non-woven mats are relatively weak and their mechanical properties must be improved to survive the winding process used in the commercial battery assembly. In addition, electrospinning is a relatively slow process, which limits the production rate of electrospun non-woven mats. As a result, electrospun nanofiber mat separators are relatively expensive and can only be used in lithium-ion batteries for special applications.

3.4. Composite membrane separators

One important method to enhance physical and chemical properties of battery separators is to introduce inorganic particles to form composite membranes. It has been reported that nanosized inorganic particles such as aluminum oxide (Al_2O_3), silicon dioxide (SiO_2) and titanium dioxide (TiO_2) can significantly improve the mechanical strength, thermal stability, and ionic conductivity of polymer electrolytes [196,197]. The addition of inorganic particles into polymer membranes can reduce their crystallinity and promote the migration of lithium ions. Inorganic particles can also lead to excellent wettability due to their high hydrophilicity and high surface area. Composite membrane separators can be classified into inorganic particle-coated composite membranes, inorganic particle-filled composite membranes, and

inorganic particle-filled non-woven mats. Table 6 shows the properties of composite membrane separators.

3.4.1. Inorganic particle-coated composite membranes

In order to improve the thermal stability and wettability of microporous polyolefin membranes, nano-sized inorganic particles were applied onto the membrane surfaces by using hydrophilic polymers as the binder. Kinouchi et al. [198] investigated the effect of inorganic particles on microporous PP-PE-PP trilayer membranes. A small amount of metal oxide particles including Al_2O_3 , SiO_2 , and zinc oxide (ZnO) were dispersed into the two PP layers of the membranes and they effectively adsorbed the impurities from the membrane materials, leading to improved battery cycling performance. In addition, these inorganic particles increased the wettability of the membranes and enhanced the retention of liquid electrolyte. PVDF-co-HFP/PEO/ Al_2O_3 [199], PVDF/PEGDA/PMMA/ Al_2O_3 / BaTiO_3 / TiO_2 [200], PVDF-co-HFP/ SiO_2 [201], PVDF-co-HFP/ AlF_3 / AlI_3 / LiF / LiI [202], poly(lithium 4-styrenesulfonate) (PLSS)/ Al_2O_3 [203], PMMA/ SiO_2 [204], Al_2O_3 /PVDF-HFP [205], PVDF-HFP/ SiO_2 [206], PVDF-HFP/ $\text{SiO}_2(\text{Li}^+)$ [207], PVDF/ SiO_2 [208] and PVDF-HFP/ Al_2O_3 [209] solutions were also used for the preparation of composite membranes by coating them onto PP and PE microporous membrane separators. In these examples, the polymer acted as a binder to bond the inorganic particle on the surface of the polyolefin membrane substrate. The resultant composite membranes exhibited good thermal stability and excellent wettability to liquid electrolytes due to the presence of inorganic particles with high surface

area. As a result, lithium-ion cells assembled with these composite membranes showed good capacity retention.

Trilayer composite membranes were prepared by coating Al_2O_3 [210] and SiO_2 [211] nanoparticle particles onto PMMA [210] and PE [211] membranes with PVDF-co-HFP as a binder. The coating solutions were prepared by mixing inorganic particles and PVDF-co-HFP binder in acetone with a filler-to-binder ratio of 9:1 (by weight). The coating solutions were applied onto microporous membrane substrates by dip coating method. The schematic of the composite membranes is shown in Figure 14. Figures 15 and 16 show the microstructures of Al_2O_3 -coated and SiO_2 -coated PE composite membranes as a function of non-solvent (*i.e.*, water) content and particle size, respectively. The membranes coated by small particles allowed higher porosity and better ionic conductivity than those with large particles. These composite membranes exhibited great thermal stability and good cell performances due to the stable microstructure of inorganic coating layers. Recently, Kim et al. [212] prepared SiO_2 -coated PE membranes by depositing SiO_2 nanoparticles onto PE membranes using the chemical vapor deposition method. The thermal stability of PE membranes was increased significantly by applying thin SiO_2 layer coating. Fang et al. [213] employed plasma treatment and SiO_2 nanoparticles to improve interfacial characteristics of PP/PE/PP membrane, and the resultant membranes exhibited enhanced ionic conductivity and cycling performance owing to their improved wettability and electrolyte uptake [213].

Some particle-coated composite membranes do not have clear trilayer structure. For example, Cho et al. [214] prepared SiO_2 particle-coated polyolefin composite membranes by an air-laid method. The SiO_2 particles were homogeneously distributed into the membranes,

filling the open pores. These SiO₂ particle-coated composite membranes were thermally stable up to 150 °C, and showed better wettability and cycling performance than the corresponding SiO₂-free membranes.

Jeong et al. [215] studied the effect of coating solution on the microporous structure of inorganic particle-coated PE membranes. PVDF-co-HFP and Al₂O₃ particles (50/50 by weight) were mixed in acetone and coated on both sides of microporous PE membranes with the presence of a nonsolvent (i.e., water). In these composite membranes, all Al₂O₃ particles were completely covered by PVDF-co-HFP. Composite membranes prepared with higher non-solvent content exhibited larger pore size and more developed pore structure, leading to the superior electrochemical performance. This is because the coating solution became immiscible with increase in non-solvent content.

Particle-coated composite membranes exhibit sufficient mechanical strength for lithium-ion battery assembly and have excellent electrochemical properties as well as good ionic conductivities. However, the increment in thickness and the reduction in porosity are inevitable consequences of the particle coating processes.

3.4.2. Inorganic particle-filled composite membranes

In addition to coating microporous membranes with inorganic particles, another simple approach to prepare composite membranes is to incorporate inorganic particles directly into the polymer matrices. For example, magnesium oxide (MgO), lithium aluminate (LiAlO₂), and Al₂O₃ particles have been filled into PVDF-co-HFP membranes [216]. SiO₂ was also introduced to the membranes prepared from poly(ethylene-co-methyl acrylate) (PE-co-MA)

[217] and PVC/PMMA blend [218]. These inorganic particles were first dispersed into the polymer solutions with selected filler-to-polymer ratios. The inorganic particle/polymer solutions were then spread over glass slides and dried to form self-standing microporous composite membranes. The electrochemical stabilities and ionic conductivities of these membranes were investigated and the membranes containing filler particles exhibited improved overall properties. However, most composite membranes prepared by this approach exhibited the formation of dense polymer phase, which inevitably caused the difficulty in filling with liquid electrolyte.

To overcome this problem, phase inversion method was applied for the fabrication of microporous PVDF-co-HFP composite membranes filled with SiO₂ [219–221], TiO₂ [222,223], and zirconium dioxide (ZrO₂) [224]. These mechanically and thermally reinforced composite membranes attained appropriate pore structure and uniform pore size while using acetone as the solvent and deionized water as the non-solvent. These microporous composite membranes showed better wettability, higher ionic conductivity, and enhanced electrochemical and interfacial stability than corresponding single-component PVDF-co-HFP membranes.

The effects of inorganic particles were investigated in detail for Al₂O₃ particle-filled PVDF [225] and PVDF-co-HFP [226] composite membranes. With increase in Al₂O₃ content, the crystallinity of the membranes decreased while the amorphous phase expanded. It was also found that the ionic conductivity and lithium ion transference number increased with increase in Al₂O₃ content because Al₂O₃ particles weakened the interaction between lithium ions and fluorine atoms in PVDF polymer chains. In addition, the membranes

containing smaller particles showed higher electrolyte retention and better cycling performance than those with large particles.

In addition to single component polymers, polymer blends have also been filled with inorganic particles to prepare composite membranes. Huang et al. [227] reported the preparation of microporous composite membranes by mixing PVDF-co-HFP/PS blend with SiO₂ particles. With increase in PS content, the porosity of the resultant membranes increased, leading to higher conductivities. Sundaram et al. [228] also described the preparation of microporous composite membranes based on PVDF-co-HFP/PVA blend and LiAlO₂ particles through the phase inversion method. The resultant composite membranes have improved electrolyte uptake and ionic conductivity because of the increased porosity and pore size caused by the addition of LiAlO₂ particles.

In addition to improving the separator properties, inorganic fillers can also be used to solve problems faced by other components in lithium-ion batteries. For example, it has been widely known that hydrogen fluoride (HF) formed by the hydrolysis of lithium hexafluorophosphate (LiPF₆) is one of main causes for the capacity fading in the cathode materials. In order to resolve this problem, Zhang et al. [229,230] used alkaline calcium carbonate (CaCO₃) to prepare composite membrane separators because it can neutralize acidic products. They prepared flexible and self-standing composite separators by a thermal pressing method. In this method, CaCO₃ and polytetrafluoroethylene (PTFE) emulsion were thoroughly mixed with a small amount of ethanol and hot-rolled to form self-standing composite membranes. These composite membranes have high ionic conductivities of 2.5 – 4 × 10⁻³ S/cm at 20 °C after absorbing liquid electrolyte. Li/graphite and Li/LiMn₂O₄ cells

using these membranes exhibited superior cycling performance at high rates. The authors argued that the superior cycling performance was attributed to the ability of alkali CaCO_3 to scavenge acidic impurities such as HF.

3.4.3. Inorganic particle-filled non-woven mats

Inorganic particles can also be introduced to non-woven mats to form composite separators. Ding et al. [231] used the electrospinning method to prepare TiO_2 -filled PVDF non-woven mats. They investigated the effect of TiO_2 particles on the morphology, crystallinity, and electrochemical properties of electrospun non-woven mats. It was found that TiO_2 -filled PVDF non-woven mats exhibited improved ionic conductivity and cycling performance compared to the non-woven mats without TiO_2 particles.

Raghavan et al. [232,233] described the preparation of electrospun PVDF-co-HFP non-woven mats with inorganic particle fillers. They incorporated nano-sized BaTiO_3 , Al_2O_3 , and SiO_2 particles into the polymer membranes by electrospinning. The resultant composite non-woven mats presented good absorption of liquid electrolyte and high electrolyte retention. The addition of inorganic particles also led to improved ionic conductivity and mechanical properties. Among the three particle fillers, BaTiO_3 gave the best electrochemical performance for the composite non-woven mats. For example, Li/LiFePO₄ cells using BaTiO_3 -filled PVDF-co-HFP non-woven mats delivered a relatively high discharge capacity of 164 mAh/g. The same research group [234] also incorporated a room-temperature ionic liquid (RTIL), n-butyl-3-methylimidazolium bis(trifluoromethanesulfonyl)imide, into BaTiO_3 -filled PVDF-co-HFP nonwoven mats. The addition of RTIL and BaTiO_3 resulted in

high ionic conductivity of 2.1×10^{-3} S/cm at room temperature and led to improved electrochemical stability. The Li/LiFePO₄ cells using the non-woven mats containing RTIL and BaTiO₃ exhibited high discharge capacity of 166 mAh/g.

Kim et al. [235] investigated the effect of SiO₂ particles on the structure and properties of electrospun PVDF-co-HFP non-woven mats. The average fiber diameter of the non-woven mats increased with increase in SiO₂ content. The addition of SiO₂ particles also inhibited the crystallization of electrospun fibers, which is beneficial for achieving higher ionic conductivity. A high specific capacity of 170 mAh/g was observed in Li/LiFePO₄ cells using 6% SiO₂-filled PVDF-co-HFP non-woven mats as the separator. Zhang et al. [236] fabricated SiO₂/PVDF composite membranes by electrospinning, and highly porous membranes with improved thermal stability and C-rate performance were obtained due to the addition of SiO₂ nanoparticles. Improvements in interfacial resistance, ionic conductivity, thermal resistance, cycling stability and rate capability were also reported by introducing SiO₂ nanoparticles in PVDF nonwoven membranes [237, 238].

In addition to PVDF and its copolymers, PAN was also used as the host membrane for inorganic particle-filled non-woven mats. Jung et al. incorporated SiO₂ into electrospun PAN non-woven mats [239]. It was found that non-woven mats containing 12% SiO₂ exhibited the smallest fiber diameter and highest porosity. After absorbing a liquid electrolyte, the non-woven mats exhibited a high ionic conductivity of 1.1×10^{-2} S/cm due to the high electrolyte uptake. In addition, electrospun non-woven mats showed good electrochemical stability when they were incorporated with 12% SiO₂.

Liang et al. [240] also introduced ionic-conductive lithium lanthanum titanate oxide (LLTO) particles into PAN non-woven mats made by electrospinning. It was found that the non-woven mats containing 15% of LLTO provided the largest electrolyte uptake and highest ionic conductivity, 1.95×10^{-3} S/cm. As a result, Li/LiFePO₄ cells using these composite non-woven mats had high discharge specific capacity and good cycling performance.

Composite non-woven mats with other unique structures have also been prepared. For example, Cho et al. [241] prepared a novel composite separator by laminating an electrospun PAN non-woven mats onto a SiO₂ or Al₂O₃ particle-filled PE/PP non-woven mat. During the preparation of this composite separator, the PE/PP non-woven was first filled by inorganic particles and then combined with the electrospun PAN membrane through hot roll press at 135 °C. Figure 17 shows laminating process and SEM images of the composite non-woven separator. This composite non-woven separator demonstrated higher porosity and air permeability than commercial separators. It was also found that the graphite/LiCoO₂ cells using this composite non-woven separator had stable cycling performance and high rate capability. In addition, no apparent thermal shrinkage was observed after exposing the composite non-woven separator at 150 °C for 1 h.

Lee et al. [242] developed a composite separator by coating PE membrane with an electrospun Al₂O₃/PVDF-co-CTFE non-woven mat (Figure 18). The coating layer was made up of electrospun fibers with diameters of 2 – 4 μm and formed greatly porous structure with thin thickness of 5 μm. The inorganic particles improved the thermal stability and wettability of the separator. The graphite/LiCoO₂ cells assembled with the composite separator showed

good capacity retention and high rate performance because of good retention capacity of liquid electrolyte.

Besides PVDF and PAN membranes, nylon 6,6 [243], polysulfonamide [244] and polyethylene terephthalate [245, 246] membranes were used to fabricate high-performance membranes by incorporating inorganic particles into the nonwoven structure. Cells using these membranes exhibited good C-rate performance and high cycling stability, which were attributed to improved interfacial resistances and higher ionic conductivities due to the effect of SiO₂ in the membranes.

As discussed above, the incorporation of inorganic particles is a promising approach to obtain high-performance lithium-ion battery separators. The inorganic particle fillers contributed to the enhanced mechanical and electrochemical properties of the membrane separators used in lithium-ion batteries.

3.5 Electrolyte membranes

When used in lithium-ion batteries, the microporous membrane, non-woven mat, and composite membrane separators discussed in previous sections need be filled with liquid electrolyte in order to transport lithium ions between the anode and cathode. Electrolyte membranes, on the other hand, are ionically conductive and can act as both separator and electrolyte between the two electrodes. There are mainly four types of electrolyte membranes: solid ceramic electrolyte, solid polymer electrolyte, gel polymer electrolyte and composite electrolyte.

Solid ceramic electrolytes are classified as crystalline electrolytes, including lithium super ionic conductor (LISICON)-type, thio-LISICON-type, Garnet-type, Perovskite-type, NASICON-type, and glass-ceramic electrolytes [247]. LISICON, with a representative structure of $\text{Li}_{14}\text{ZnGe}_4\text{O}_{16}$, has been extensively studied for use as solid ceramic electrolytes in lithium-ion batteries. LISICON has a wide electrochemical stability window and can be used in high-temperature batteries due to its excellent thermal stability and near-zero vapor pressure [247, 248]. However, the interface between solid LISiCON and the electrodes is relatively poor due to the poor solid-to-solid connection. Recently, Kim et al. [248] coated an ionic liquid (N-propyl-N-methylpyrrolidinium bisfluorosulfonylimide, $\text{PYR}_{13}^+\text{FSI}^-$) onto a solid LISICON electrolyte to improve the electrolyte-electrode interface, which led to good cycle and C-rate performance at 80 °C. In recent years, the ionic conductivity of LISICON electrolyte was enhanced by replacing oxide with sulfur in the structure, and the resultant electrolyte was referred to as thio-LISICON. Inada et al. [249] fabricated solid-state lithium batteries by using a thio-LISICON ($\text{Li}_{3.25}\text{Ge}_{0.25}\text{P}_{0.75}\text{S}_4$) electrolyte and achieved good charge-discharge characteristics without any apparent capacity fading in eight cycles. The representative structures of Garnet-type, Perovskite-type, and NASICON-type electrolytes are $\text{Li}_5\text{La}_3\text{M}_2\text{O}_{12}$ (M: Ta, Nb), $\text{Li}_{3x}\text{La}_{2/3-x}\text{TiO}_3$, and $\text{LiA}_2^{\text{IV}}(\text{PO}_4)_3$ (A^{IV} : Ti, Zr, Ge, Hf), respectively [247, 250, 251]. There are many types of glass-ceramic electrolytes, and examples include $\text{Li}_{1.4}\text{Al}_{0.4}\text{Ti}_{1.6}(\text{PO}_4)_3$, $\text{Li}_{1.4}\text{Al}_{0.4}\text{Ti}_{1.6}(\text{PO}_4)_3$, and $\text{Li}_7\text{P}_3\text{S}_{11}$ [252-254]. All these solid ceramic electrolytes have high conductivities of 10^{-3} S/cm or even higher [252-256]. However, one major disadvantage of these solid ceramic electrolytes is their brittleness, which makes it challenging to use them directly in lithium-ion batteries.

Solid polymer electrolytes are soft and are composed of high-molecular weight polymer hosts and lithium salts. In a typical solid polymer electrolyte, the polymer host acts as a solid solvent and dissolves lithium salts. PEO, PAN, PVDF, and PMMA, are commonly used polymer hosts for solid polymer electrolytes. One major weakness of solid polymer electrolytes is their relatively low conductivities because the crystalline phase of the polymer restricts ionic transport. Different approaches have been reported to decrease the crystallinity of solid polymer electrolytes, such as adding plasticizers and using copolymer structures [257-260]. For example, Sukeshini et al. [257] used dibutyl phthalate as a plasticizer and increased the conductivity of PEO based polymer electrolyte from 7.1×10^{-7} S/cm to 6×10^{-4} S/cm. Ji et al. [259] utilized poly(ethylene oxide)-block-polyethylene (PEO-block-PE) copolymer to prepare solid polymer electrolytes, where PEO block acts as the conductive phase and PE acts as a reinforcement component. The resultant solid polymer electrolytes presented improved conductivity of 3.2×10^{-4} S/cm. In another study, Gavelin et al. [260] prepared copolymer consisting of methacrylate backbones and ethylene oxide side chains and they achieved an ionic conductivity of 10^{-5} S/cm. Solid polymer electrolytes have the advantages of high safety, good stability, and thin film manufacturability. However, for practical battery applications, most solid polymer electrolytes still have unsatisfactory ionic conductivities.

Compared with solid polymer electrolytes, gel polymer electrolytes have significantly higher ionic conductivity. They also possess wide electrochemical window, high thermal stability and good compatibility with electrodes. The charge-transport mechanism in gel polymer electrolytes is similar to that in liquid electrolytes. The motion and rearrangement of

polymer chains also contribute to the ionic transport as well. There are different methods to prepare gel electrolytes such as bellcore process, in which nanoporous membranes are prepared through a liquid extraction/activation technique, solvent casting, phase inversion, and electrospinning. Polymers that are commonly used for making gel polymer electrolytes include but are not limited to PEO, PVDF, PAN, and PMMA. Low molecular weight polyethers or organic solvents are often added to form gel polymer electrolytes, which have reduced crystallinity and increased polymer segmental mobility as compared with solid polymer electrolytes [261, 262]. Sekhon et al. [263] prepared PVDF based gel polymer electrolytes by using ethylene carbonate, propylene carbonate and dimethyl acetamide as a ternary solvent, and they achieved relatively high ionic conductivity of about 10^{-4} S/cm at 20 °C. Choi et al. [264] prepared PAN based electrolytes with high ionic conductivity of around 10^{-3} S/cm⁻¹ and wide electrochemical stability window up to 4.5 V. Saunier et al. [265] prepared gel polymer electrolytes by filling PVDF microporous membranes with a liquid electrolyte (1 M LiPF₆ in EC, DMC, DEC) and the ionic conductivities of these electrolytes increased by increasing the porosity of the microporous membranes. Several groups have reported PVDF based gel polymer electrolytes produced by electrospinning [266, 267, 264, 268] and the conductivities of these electrolytes were in the range of 10^{-3} S/cm.

The effect of interfacial compatibility between gel polymer electrolytes and the electrodes was investigated by Cao and coworkers [269]. It was found that the overpotential caused by ohmic polarization had major effect on the electrode capacities, and the improvement of the interfacial compatibility between gel polymer electrolytes and the electrodes could decrease the surface film resistance, bulk resistance, charge transfer

resistance and diffusion resistance, thereby resulting in decreased ohmic polarization of the cells [269]. Rao et al. [270] prepared electrospun PAN/PMMA based gel polymer electrolytes. These PAN/PMMA based electrolytes exhibited better cycling and C-rate performance than PAN electrolytes due to their higher ionic conductivities and lower interfacial resistances. Mechanical and electrochemical stabilities are also the key issues for gel polymer electrolytes. Blending different polymers may help address these issues. Flora et al. [271] reported PAN/PMMA based gel polymer electrolytes by the solution casting technique and their results showed that the electrolyte containing PAN/PMMA (75:25 wt.%) was thermally stable until 200 °C. Subramania et al. [272] and Gopalan et al. [273] blended PAN with PVDF to prepare gel polymer electrolytes, and it was found that the introduction of PAN led to reduced dendrite growth, higher mechanical stability and improved interfacial characteristics compared with PVDF based electrolytes [273]. Zhu et al. [4] combined PVDF nanofibers and lithium polyvinyl alcohol oxalate borate (LiPVAOB) to obtain gel polymer electrolytes with high safety and good mechanical stability. Other examples of blend-based gel polymer electrolytes include PVDF-HFP/PEGDMA [274], PVDF/polydiphenylamine (PDPA) [275], PVDF-HFP/PAN [272], PVDF/PVC [276], PVDF/PDMS [277] and PVDF/polysulfone (PSF) [278].

Composite electrolytes can be obtained by the introduction of inorganic fillers to solid polymer electrolytes or gel polymer electrolytes. SiO₂, TiO₂, MgO and Al₂O₃ are commonly used inorganic fillers for improving the ionic conductivity and interfacial properties of the electrolytes [279-285]. Liao et al. [286] prepared fumed SiO₂ containing poly(butyl methacrylate-styrene)-based electrolytes by using the phase inversion technique. The

resultant composite polymer electrolytes have high ionic conductivity of 2.15×10^{-3} S/cm and good electrochemical stability of up to 5.2 V. Liu et al. [287] investigated Li dendrite growth and they found that the presence of nano-SiO₂ contributed to the suppression of dendrite formation due to improved conductivity and decreased interfacial resistance. Yang et al. [288] prepared composite polymer electrolytes based on PVDF and mesoporous-SiO₂ fillers. Cycling and C-rate performance was improved by the introduction of SiO₂ fillers, which helped retain more electrolyte in the structure. Cao et al. [289] used PVDF-HFP gel electrolyte with TiO₂-PMMA hybrid additive to prepare composite polymer electrolytes. These composite membranes exhibited increased electrolyte uptake and ionic conductivity, leading to improved cycle performance. It was also found that the dispersibility of TiO₂ nanoparticles had major effect on the performance of the composite membranes. In general, the well-dispersed TiO₂ nanoparticles were able to provide more favorable lithium ionic conduction pathways [290]. In another study, Cao et al. [291] found that TiO₂-PMMA nanohybrid-added PVDF-HFP composite polymer electrolyte exhibited improved pore distribution, electrolyte uptake and ionic conductivity. Furthermore, the C-rate performance was enhanced owing to the decreased interfacial resistance.

Recently, a new way to improve the ionic conductivity of polymer electrolytes has been introduced by preparing ionic liquid based electrolytes. Ionic liquids are non-volatile, non-flammable molten salts with low melting points. They exhibit high ionic conductivity, high thermal and chemical stability, wide electrochemical window, and low toxicity [292]. Cheruvally et al. [292] prepared ionic liquid-contained PVDF-HFP electrolytes and achieved good electrochemical properties. Liao et al. [293] added ionic liquid (LiTFSI in N-butyl-N-

methyl pyrrolidinium bis(trifluoromethanesulfonyl)imide (PYR₁₄TFSI) to SiO₂/PE/polymethyl methacrylate–acrylonitrile–vinyl acetate (PMMA-AN-VAc) and Al₂O₃/PMMA–AN–VAc, and the obtained composite electrolytes had high ionic conductivity, wide stability window, enhanced thermal stability. Zhai et al. [294] used ionic liquid, 1-butyl-3-methylimidazolium tetrafluoroborate ([BMIM]BF₄), to plasticize PVDF-HFP/PMMA polymer electrolytes and achieved a high conductivity of 1.4×10^{-3} S/cm with good thermal stability, good interfacial stability and stable potential window of up to 4.5 V.

Ion-exchange membranes swollen with organic non-aqueous solvent have also been studied for use as both separator and electrolyte. Cai et al. [295] prepared lithiated perfluorinated sulfonic ion-exchange membranes by swelling them with an organic non-aqueous solvent. These ion-exchange membranes not only showed high thermal and mechanical stabilities, but also exhibited good interfacial compatibility with the electrodes in lithium-ion batteries. Liu et al. [296] investigated the ionic conductivities of lithiated perfluorinated sulfonic acid ion-exchange membranes by swelling them in different nonaqueous organic solvents. The ionic conductivities of the resultant membranes were found to be determined by the ionomer equivalent weight, solvent uptake, solvent viscosity, solvent constant, and temperature. Liu et al. [297] also swelled lithiated perfluorinated sulfonic acid ion-exchange membranes with organic non-aqueous solvent to overcome the capacity fading of LiMn₂O₄ cathode.

4. Summary and outlook

Separator is a crucial component in rechargeable lithium-ion battery. The main role of the separator is to prevent physical contact between the positive and negative electrodes of the battery and to prevent internal short while serving as the electrolyte reservoir to enable ionic transport. The ideal separator should have large electrolyte uptake for lowering the cell internal resistance, have extremely thin thickness with strong mechanical strength, be electrochemically and structurally stable, and have highly porous structure with great tortuosity to prevent the growth of dendritic lithium. In addition, the separator should be able to shut the battery down when overheating occurs in order for battery safety. However, practical separators cannot simultaneously possess all these ideal properties, and it becomes extremely important to balance different separator properties to achieve high-performance batteries. The actual structure and property requirements of separators depend on the particular battery application requiring specific properties.

As stated above, there is not a single separator that can meet all requirements for different battery applications. Currently, microporous polyolefin membranes are the most commonly used separator for rechargeable lithium-ion batteries. Several microporous multilayer membranes have been used in commercial lithium ion batteries, addressing the issues raised from the drawbacks of microporous monolayer membranes. However, microporous polyolefin membranes can still be improved in terms of conductivity, thermal stability, and wettability for the higher performance of lithium-ion batteries.

Microporous membranes have been modified by using various techniques such as plasma, UV irradiation, Gamma ray, electron beam irradiation, and polymer coating.

Modified microporous membranes provide the improved properties including mechanical strength, thermal stability, wettability, and ionic conductivity.

Non-woven mats, especially electrospun non-woven mats, have also been used as the separators in lithium-ion batteries. Electrospun non-woven mats show many advantages as battery separators, including small pore size, high porosity, large surface area, interconnected open structure, and high permeability. However, electrospun non-woven mats have relatively weak mechanical properties compared to microporous membranes and modified microporous membranes. In order to address these issues, electrospun non-woven mats with enhanced mechanical properties and thermal stability can be obtained by using polymeric materials with high mechanical strength and melting temperature. Furthermore, considering the disadvantages of electrospinning such as safety, slow production, and high cost, new production techniques may be offered to produce non-woven mats with low cost and enhanced performance.

Composite membrane separators combined with multiple membranes and unique materials, such as inorganic particles, could be promising for next-generation lithium-ion batteries. Incorporation of inorganic particles into the membranes is an attractive method to obtain high-performance lithium-ion battery separators with advanced physical and electrochemical properties. However, it is still difficult to combine inorganic particles with organic materials effectively. For successful development, the novel composite membrane separators should be attempted by understanding the relationship between organic and inorganic materials. Furthermore, it is very important to optimize various properties of

battery separators to achieve high battery performance while maintaining high safety and low cost.

When used in lithium-ion batteries, microporous membrane, non-woven mat, and composite membrane separators must be filled with liquid electrolyte in order to transport lithium ions between the anode and cathode. Electrolyte membranes, on the other hand, are ionically conductive and can act as both separator and electrolyte between the two electrodes. They are suitable for flexible batteries and/or solid state batteries with high safety. However, work is needed to improve the ionic conductivity and mechanical properties of these membranes.

In the future, battery separators would demand unique properties including basic requirements as there has been a continued demand for advanced batteries. Unique techniques such as self-assembly and atomic layer deposition can also be applied to prepare advanced separators used in lithium-ion batteries. Consequently, further research for the development of new separator structures is needed to achieve advanced batteries with excellent performance.

Acknowledgements

The authors acknowledge the financial support from Advanced Transportation Energy Center and ERC Program of the National Science Foundation under Award Number EEC-08212121.

5. References

- [1] M.R. Palacín, *Chemical Society Reviews* 38 (2009) 2565.
- [2] K.M. Abraham, *Electrochimica Acta* 38 (1993) 1233.
- [3] P. Arora, Z. Zhang, *Chemical Reviews* 104 (2004) 4419.
- [4] Y. Zhu, S. Xiao, Y. Shi, Y. Yang, Y. Hou, Y. Wu, *Advanced Energy Materials* 4 (2014) 1.
- [5] J.R. Kim, S.W. Choi, S.M. Jo, W.S. Lee, B.C. Kim, *Journal of The Electrochemical Society* 152 (2005) A295.
- [6] M. Yang, J. Hou, *Membranes* 2 (2012) 367.
- [7] M.B. Johnson, G.L. Wilkes, *Journal of Applied Polymer Science* 83 (2002) 2095.
- [8] M.B. Johnson, G.L. Wilkes, *Journal of Applied Polymer Science* 84 (2002) 1762.
- [9] Johnson, M.B., Wilkes, G.L., *Journal of Applied Polymer Science* 81 (2001) 2944.
- [10] P. Jacoby, C.W. Bauer, S.R. Clingman, W.T. Tapp, Oriented polymeric microporous films, U.S. Patent 5317035, 1994.
- [11] H. Higuchi, K. Matsushita, M. Ezo, T. Shinomura, Porous film, process for producing the same and use of the same, U.S. Patent 5385777, 1995.
- [12] H. Sogo, Separator for a battery using an organic electrolytic solution and method for preparing the same, U.S. Patent 5641565, 1997.
- [13] C. Chandavas, M. Xanthos, K.K. Sirkar, C. Gogos, Preparation of microporous films from immiscible blends via melt processing and stretching, U.S. Patent 6824680, 2004.
- [14] H.S. Bierenbaum, R.B. Isaacson, M.L. Druin, S.G. Plovan, *Ind. Eng. Chem. Prod. Res. Develop.* 13 (1974) 2.

- [15] A. Hashimoto, K. Yagi, H. Mantoku, Porous film of high molecular weight polyolefin and process for producing same, U.S. Patent 6048607, 2000.
- [16] S. Nagou, S. Nakamura, Microporous film and process for production thereof, U.S. Patent 4791144, 1988.
- [17] M. Xu, J. Guan, X. Sun, W. Wu, W. Zhu, X. Zhang, Z. Ma, Q. Han, S. Liu, Polypropylene microporous film, U.S. Patent 5134174, 1992.
- [18] N. Brough, A.H. Fawcett, W. Burns, S. Harrod, *Polymer* 37 (1996) 537.
- [19] H.M. Fisher, C.G. Wensley, Polypropylene microporous membrane for battery separator, U.S. Patent 6368742, 2002.
- [20] S.Y. Lee, B.I. Ahn, S.G. Im, S.Y. Park, H.S. Song, Y.J. Kyung, High crystalline polypropylene microporous membrane, multi-component microporous membrane and methods for preparing the same, U.S. Patent 6830849, 2004.
- [21] H.M. Fisher, D.E. Leone, J.J. Lowery, Microporous membranes having increased pore densities and process for making the same, U.S. Patent 5013439, 1991.
- [22] W.C. Yu, M.W. Geiger, Shutdown, bilayer battery separator, U.S. Patent 5565281, 1996.
- [23] W.C. Yu, Methods of making cross-ply microporous membrane battery separator and the battery separators made thereof, U.S. Patent 5667911, 1997.
- [24] W.C. Yu, Shutdown, trilayer battery separator, U.S. Patent 5691077, 1997.
- [25] T.H. Yu, Trilayer battery separator, U.S. Patent 6080507, 2000.
- [26] W.C. Yu, Continuous methods of making microporous battery separators, U.S. Patent 6878226, 2005.

- [27] T. Sarada, L.C. Sawyer, M.I. Ostler, *Journal of Membrane Science* 15 (1983) 97.
- [28] S.S. Zhang, *Journal of Power Sources* 164 (2007) 351.
- [29] X. Zhang, G.P. Rumierz, K.F. Humiston, C.E. Haire, T.S. Fields, M.A. Braswell, R.A. Proctor, Biaxially oriented porous membranes, composites and methods of manufacture and use, U.S. Patent 20010223486, 2011.
- [30] M.L. Druin, J.T. Loft, S.G. Plovon, Novel open-celled microporous film, U.S. Patent 3801404, 1974.
- [31] R.B. Isaacson, H.S. Bierenbaum, Process for preparing microporous film, U.S. Patent 3558764, 1971.
- [32] H.S. Bierenbaum, L.R. Daley, D. Zimmerman, I.L. Hay, Process for preparing a thermoplastic microporous film involving a cold stretching step and multiple hot stretching steps, U.S. Patent 3843761, 1974.
- [33] E.A.G. Hamer, Process for preparing microporous polyethylene film by uniaxial cold and hot stretching, U.S. Patent 4620956, 1986.
- [34] H. Kurauchi, T. Akazawa, A. Kawabata, Porous multi-layer film, U.S. Patent 5691047, 1997.
- [35] R.E. Kesting, *Synthetic polymeric membranes: a structural perspective*, 2nd ed., Wiley, New York, 1985.
- [36] N. Kaimai, K. Takita, K. Kono, H. Funaoka, Method of producing highly permeable microporous polypropylene membrane, U.S. Patent 6153133, 2000.
- [37] P. Jacoby, C.W. Bauer, Oriented porous polypropylene films, U.S. Patent 4975469, 1990.

- [38] K. Takita, K. Kono, T. Takashima, K. Okamoto, Microporous polyolefin membrane and method of producing same, U.S. Patent 5051183, 1991.
- [39] P. Jacoby, C.W. Bauer, S.R. Clingman, W.T. Tapp, Oriented polymeric microporous films, U.S. Patent 5176953, 1993.
- [40] L.K. Yankov, S.K. Filipova, I.Y. Zlatanov, E.B. Budevski, Composition for microporous separators and method for its preparation, U.S. Patent 4959396, 1990.
- [41] J.S. Oh, Y. Kang, D.W. Kim, *Electrochimica Acta* 52 (2006) 1567.
- [42] E. Kessler, T. Batzilla, F. Wechs, F. Wiese, Integrally asymmetrical polyolefin membrane, U.S. Patent 6497752, 2002.
- [43] E. Kessler, T. Batzilla, F. Wechs, F. Wiese, Method for producing an intergrally asymmetrical polyolefin membrane, U.S. Patent 6375876, 2002.
- [44] J.J. Kim, S.S. Kim, J.R. Hwang, S.B. Suh, Process for the preparation of porous polyolefin separation membranes via thermally-induced phase separation, U.S. Patent 5250240, 1993.
- [45] H. Strathmann, K. Kock, *Desalination* 21 (1977) 241.
- [46] X. He, Q. Shi, X. Zhou, C. Wan, C. Jiang, *Electrochimica Acta* 51 (2005) 1069.
- [47] S.S. Zhang, M.H. Ervin, K. Xu, T.R. Jow, *Solid State Ionics* 176 (2005) 41.
- [48] S.S. Zhang, K. Xu, D.L. Foster, M.H. Ervin, T.R. Jow, *Journal of Power Sources* 125 (2004) 114.
- [49] J. Song, M. H. Ryou, B. Son, J. N. Lee, D. J. Lee, Y. M. Lee, J. W. Choi, J. K. Park, *Electrochimica Acta* 85 (2012) 524.

- [50] D. Djian, F. Alloin, S. Martinet, H. Lignier, J.Y. Sanchez, *Journal of Power Sources* 172 (2007) 416.
- [51] G. Venugopal, J. Moore, J. Howard, S. Pendalwar, *Journal of Power Sources* 77 (1999) 34.
- [52] M.S. Wu, P.C.J. Chiang, J.C. Lin, Y.S. Jan, *Electrochimica Acta* 49 (2004) 1803.
- [53] C.T. Love, *Journal of Power Sources* 196 (2011) 2905.
- [54] D.W. Ihm, J.G. Noh, J.Y. Kim, *Journal of Power Sources* 109 (2002) 388.
- [55] A. Bottino, G. Camera-Roda, G. Capannelli, S. Munari, *Journal of Membrane Science* 57 (1991) 1.
- [56] F. Boudin, X. Andrieu, C. Jehoulet, I.I. Olsen, *Journal of Power Sources* 81-82 (1999) 804.
- [57] J. Saunier, F. Alloin, J. Sanchez, G. Caillon, *Journal of Power Sources* 119–121 (2003) 454.
- [58] A. Magistris, P. Mustarelli, F. Parazzoli, E. Quartarone, P. Piaggio, A. Bottino, *Journal of Power Sources* 97-98 (2001) 657.
- [59] D. Djian, F. Alloin, S. Martinet, H. Lignier, *Journal of Power Sources* 187 (2009) 575.
- [60] G.L. Ji, B.K. Zhu, Z.Y. Cui, C.F. Zhang, Y.Y. Xu, *Polymer* 48 (2007) 6415.
- [61] Z. Jiang, B. Carroll, K.M. Abraham, *Electrochimica Acta* 42 (1997) 2667.
- [62] J.A. Morehouse, L.S. Worrel, D.L. Taylor, D.R. Lloyd, B.D. Freeman, D.F. Lawler, *Journal of Porous Materials* 13 (2006) 61.
- [63] H.S. Min, J.M. Ko, D.W. Kim, *Journal of Power Sources* 119-121 (2003) 469.

- [64] B. Jung, J.K. Yoon, B. Kim, H.W. Rhee, *Journal of Membrane Science* 246 (2005) 67.
- [65] B. Jung, *Journal of Membrane Science* 229 (2004) 129.
- [66] F. Groce, F. Gerace, G. Dautzemberg, S. Passerini, G.B. Appetecchi, B. Scrosati, *Electrochimica Acta* 39 (1994) 2187.
- [67] G.B. Appetecchi, F. Croce, B. Scrosati, *Journal of Power Sources* 66 (1997) 77.
- [68] O. Bohnke, G. Frand, M. Rezrazi, C. Rousselot, C. Truche, *Solid State Ionics* 66 (1993) 97.
- [69] M.H. Lee, H.J. Kim, E. Kim, S.B. Rhee, M.J. Moon, *Solid State Ionics* 85 (1996) 91.
- [70] G.B. Appetecchi, F. Croce, B. Scrosati, *Electrochimica Acta* 40 (1995) 991.
- [71] A. Gopalan, P. Santhosh, K. Manesh, J. Nho, S. Kim, C. Hwang, K. Lee, *Journal of Membrane Science* 325 (2008) 683.
- [72] A. Manuel Stephan, K.S. Nahm, *Polymer* 47 (2006) 5952.
- [73] A. Magistris, E. Quartarone, P. Mustarelli, Y. Saito, H. Kataoka, *Solid State Ionics* 152 (2002) 347.
- [74] Q. Shi, M. Yu, X. Zhou, Y. Yan, C. Wan, *Journal of Power Sources* 103 (2002) 286.
- [75] S.S. Zhang, K. Xu, D.L. Foster, M.H. Ervin, T.R. Jow, *Journal of Power Sources* 125 (2004) 114.
- [76] G. Wu, H.Y. Yang, H.Z. Chen, F. Yuan, L.G. Yang, M. Wang, R.J. Fu, *Materials Chemistry and Physics* 104 (2007) 284.
- [77] Y.H. Liao, D.Y. Zhou, M.M. Rao, W.S. Li, Z.P. Cai, Y. Liang, C.L. Tan, *Journal of Power Sources* 189 (2009) 139.

- [78] D.Y. Zhou, G.Z. Wang, W.S. Li, G.L. Li, C.L. Tan, M.M. Rao, Y.H. Liao, *Journal of Power Sources* 184 (2008) 477.
- [79] A. Subramania, N.T.K. Sundaram, G.V. Kumar, *Journal of Power Sources* 153 (2006) 177.
- [80] B. Jung, J.K. Yoon, B. Kim, H.W. Rhee, *Journal of Membrane Science* 243 (2004) 45.
- [81] I. Nicotera, L. Coppola, C. Oliviero, M. Castriota, E. Cazzanelli, *Solid State Ionics* 177 (2006) 581.
- [82] D.J. Lin, C.L. Chang, C.K. Lee, L.P. Cheng, *European Polymer Journal* 42 (2006) 2407.
- [83] T. Ma, Z. Cui, Y. Wu, S. Qin, H. Wang, F. Yan, N. Han, J. Li, *Journal of Membrane Science* 444, (2013) 213.
- [84] H.J. Rhoo, H.T. Kim, J.K. Park, T.S. Hwang, *Electrochimica Acta* 42 (1997) 1571.
- [85] Z. Tian, W. Pu, X. He, C. Wan, C. Jiang, *Electrochimica Acta* 52 (2007) 3199.
- [86] Z. Ren, Y. Liu, K. Sun, X. Zhou, N. Zhang, *Electrochimica Acta* 54 (2009) 1888.
- [87] Z.L. Wang, Z.Y. Tang, *Electrochimica Acta* 49 (2004) 1063.
- [88] J.D. Jeon, B.W. Cho, S.Y. Kwak, *Journal of Power Sources* 143 (2005) 219.
- [89] N.S. Choi, Y.G. Lee, J.K. Park, J.M. Ko, *Electrochimica acta* 46 (2001) 1581.
- [90] C.M. Costa, J.L. Gomez Ribelles, S. Lanceros-Méndez, G.B. Appetecchi, B. Scrosatie, *Journal of Power Sources* 245 (2014) 779.
- [91] H. Li, C. E. Lin, J. L. Shi, X. T. Ma, B. Ku, L. P. Zhu, *Electrochimica Acta* 115 (2014) 317.

- [92] H. Li, H. Zhang, Z. Y. Liang, Y. M. Chen, B. K. Zhu, L. P. Zhu, *Electrochimica Acta* 116 (2014) 413-420.
- [93] C. M. Costa, V. Sencadas, J. G. Rocha, M. M. Silva, S. Lanceros-Méndez, *Journal of Solid State Electrochemistry* 17 (2013) 861.
- [94] R.M. Janmey, Electrochemical cell with reinforced separator, U.S. Patent 6828061, 2004.
- [95] F.C. Arrance, C. Mesa, Battery separator, U.S. Patent 3542596, 1970.
- [96] Y. Shinohara, Y. Tsujimoto, T. Nakano, Non-woven electrolyte battery separator, U.S. Patent 6447958, 2002.
- [97] R.W. Pekala, M. Khavari, Freestanding microporous separator including a gel-forming polymer, U.S. Patent 20020001753, 2002.
- [98] H.T. Taskier, Hydrophilic polymer coated microporous membranes capable of use as a battery separator, U.S. Patent 4359510, 1982.
- [99] T. Hashimoto, H. Totsuka, M. Takahata, M. Takanashi, Y. Oota, K. Sano, Separator for power storage device, U.S. Patent 20100316912, 2010.
- [100] S.A. Carlson, Microporous separators, U.S. Patent 20040185335, 2004.
- [101] Q. Ying, S.A. Carlson, T.A. Skotheim, Protective coating for separators for electrochemical cells, U.S. Patent 6194098, 2001.
- [102] C.D. Lang, T.J. Faircloth, Apparatus and method for solution coating thin layers, U.S. Patent 20110086164, 2011.
- [103] W.C. Rice, J.P. Puglia, High performance composite membrane, U.S. Patent 6536605, 2003.

- [104] J.H. Kim, J.S. Yu, J.H. Choi, Rechargeable lithium battery using separator partially coated with gel polymer, U.S. Patent 8003263, 2011.
- [105] H.S. Choi, Y.K. Lee, C.H. Park, B.Y. Choi, K.J. Lee, Manufacturing method of film having micro-pattern thereon and film manufactured thereby, U.S. Patent 20100055401, 2010.
- [106] H.S. Jeong, J.H. Kim, S.Y. Lee, *Journal of Materials Chemistry* 20 (2010) 9180.
- [107] H.S. Jeong, E.S. Choi, J.H. Kim, S.Y. Lee, *Electrochimica Acta* 56 (2011) 5201.
- [108] J.T. Lundquist, C.B. Lundsager, N.I. Palmer, H.J. Troffkin, Battery separator, U.S. Patent 4650730, 1987.
- [109] W.C. Yu, S.E. Hux, Method of making a trilayer battery separator, U.S. Patent 5952120, 1999.
- [110] R.W. Callahan, R.W. Call, K.J. Harleson, T.H. Yu, Battery separators with reduced splitting propensity, U.S. Patent 6602593, 2003.
- [111] Y.M. Lee, J.W. Kim, N.S. Choi, J.A. Lee, W.H. Seol, J.K. Park, *Journal of Power Sources* 139 (2005) 235.
- [112] Y.B. Jeong, D.W. Kim, *Journal of Power Sources* 128 (2004) 256.
- [113] Y.M. Lee, N.S. Choi, J.A. Lee, W.H. Seol, K.Y. Cho, H.Y. Jung, J.W. Kim, J.K. Park, *Journal of Power Sources* 146 (2005) 431.
- [114] P. Periasamy, K. Tatsumi, M. Shikano, T. Fujieda, Y. Saito, T. Sakai, M. Mizuhata, A. Kajinami, S. Deki, *Journal of Power Sources* 88 (2000) 269.
- [115] H.S. Kim, P. Periasamy, S.I. Moon, *Journal of Power Sources* 141 (2005) 293.

- [116] J.Y. Sohn, J.S. Im, S.J. Gwon, J.H. Choi, J. Shin, Y.C. Nho, *Radiation Physics and Chemistry* 78 (2009) 505.
- [117] J.Y. Sohn, S.J. Gwon, J.H. Choi, J. Shin, Y.C. Nho, *Nuclear Instruments and Methods in Physics Research Section B* 266 (2008) 4994.
- [118] M.K. Song, Y.T. Kim, J.Y. Cho, B.W. Cho, B.N. Popov, H.W. Rhee, *Journal of Power Sources* 125 (2004) 10.
- [119] H. Li, X.T. Ma, J.L. Shi, Z.K. Yao, B.K. Zhu, L.P. Zhu, *Electrochimica Acta* 56 (2011) 2641.
- [120] G. Chen, T.J. Richardson, *Electrochemical and Solid-State Letters* 7 (2004) A23.
- [121] S.L. Li, L. Xia, H.Y. Zhang, X.P. Ai, H.X. Yang, Y.L. Cao, *Journal of Power Sources* 196 (2011) 7021.
- [122] S.L. Li, X.P. Ai, H.X. Yang, Y.L. Cao, *Journal of Power Sources* 189 (2009) 771.
- [123] Y. Huai, J. Gao, Z. Deng, J. Suo, *Ionics* 16 (2010) 603.
- [124] J.H. Park, W. Park, J.H. Kim, D. Ryoo, H.S. Kim, Y.U. Jeong, D.W. Kim, S.Y. Lee, *Journal of Power Sources* 196 (2011) 7035.
- [125] M. Alcoutlabi, H. Lee, J.V. Watson, X. Zhang, *J. Mater. Sci.* 48 (n.d.) 2690.
- [126] H. Lee, M. Alcoutlabi, J.V. Watson, X. Zhang, *J. Polym. Sci. Part B: Polym. Physics* 51 (n.d.) 349.
- [127] H.P. Zhang, P. Zhang, Z.H. Li, M. Sun, Y.P. Wu, H.Q. Wu, *Electrochemistry Communications* 9 (2007) 1700.
- [128] T. Tanaka, H. Yamaguchi, N. Takimoto, M. Yamachita, S. Hamamoto, Battery separator, process for producing the same, and alkaline battery, U.S. Patent 6821680, 2004.

- [129] Y. Takeuchi, M. Kawabe, H. Yamazaki, M. Kaneko, G. Anan, K. Sato, Sulfur containing atomic group introduced porous article, U.S. Patent 6171708, 2001.
- [130] S. Senyarich, P. Viaud, Method of forming a separator for alkaline electrolyte secondary electric cell, U.S. Patent 6042970, 2000.
- [131] M. Urairi, T. Tachibana, K. Matsumoto, T. Shinomura, H. Iida, K. Kawamura, S. Yano, O. Ishida, Process for producing a wind-type alkaline secondary battery, U.S. Patent 5558682, 1996.
- [132] M. Nasef, *Progress in Polymer Science* 29 (2004) 499.
- [133] J.Y. Kim, D.Y. Lim, *Energies* 3 (2010) 866.
- [134] J.Y. Kim, Y. Lee, D.Y. Lim, *Electrochimica Acta* 54 (2009) 3714.
- [135] J.L. Gineste, G. Pourcelly, *Journal of Membrane Science* 107 (1995) 155.
- [136] J.M. Ko, B.G. Min, D.W. Kim, K.S. Ryu, K.M. Kim, Y.G. Lee, S.H. Chang, *Electrochimica Acta* 50 (2004) 367.
- [137] K. Gao, X. Hu, T. Yi, C. Dai, *Electrochimica Acta* 52 (2006) 443.
- [138] J.Y. Lee, B. Bhattacharya, Y.C. Nho, J.K. Park, *Nuclear Instruments and Methods in Physics Research Section B* 267 (2009) 2390.
- [139] J.Y. Lee, Y.M. Lee, B. Bhattacharya, Y.C. Nho, J.K. Park, *Electrochimica Acta* 54 (2009) 4312.
- [140] K.J. Kim, Y.H. Kim, J.H. Song, Y.N. Jo, J.S. Kim, Y.J. Kim, *Journal of Power Sources* 195 (2010) 6075.
- [141] C.R. Jarvis, W.J. Macklin, A.J. Macklin, N.J. Mattingley, E. Kronfli, *Journal of Power Sources* 97 (2001) 664.

- [142] K.U. Jeong, H.D. Chae, C.I. Lim, H.K. Lee, J.H. Ahn, C. Nah, *Polymer International* 59 (2009) 249.
- [143] M.K. Song, Y.T. Kim, Y.T. Kim, B.W. Cho, B.N. Popov, H.W. Rhee, *Journal of The Electrochemical Society* 150 (2003) A439.
- [144] Y. Lee, M. H. Ryou, M. Seo, J. W. Choi, Y. M. Lee, *Electrochimica Acta* 113 (2013) 433.
- [145] M. H. Ryou, D. J. Lee, J. N. Lee, Y. M. Lee, J. K. Park, J. W. Choi, *Advanced Energy Materials* 2 (2012) 645.
- [146] M. H. Ryou, Y. M. Lee, J. K. Park, J. W. Choi, *Advanced Materials* 23 (2011) 3066.
- [147] L. F. Fang, J. L. Shi, B. Ku, L. P. Zhu, *Journal of Membrane Science* 448 (2013) 143.
- [148] S. M. Kang, M. H. Ryou, J. W. Choi, H. Lee, *Chemistry of Materials* 24 (2012) 3481.
- [149] H. Li, X. T. Ma, J. L. Shi, Z. K. Yao, B. K. Zhu, L. P. Zhu, *Electrochimica Acta* 56 (2011) 2641.
- [150] J. L. Shi, L. F. Fang, H. Li, H. Zhang, B. K. Zhu, L. P. Zhu, *Journal of Membrane Science* 437 (2013) 160.
- [151] J. Y. Sohn, J. S. Im, J. Shin, Y. C. Nho, *Journal of Solid State Electrochemistry* 16 (2012) 2 551.
- [152] M. Tanaka, H. Yamazaki, Y. Kondo, K. Takahashi, T. Takase, S. Oota, *Battery separator*, U.S. Patent 6586137, 2003.
- [153] J. Zucker, *Melt blown battery separator*, U.S. Patent 6692868, 2004.

- [154] Y. Sudou, H. Suzuki, S. Nagami, K. Ikuta, T. Yamamoto, S. Okijima, S. Suzuki, H. Ueshima, Separator for battery and lithium ion battery using the same, U.S. Patent 20060073389, 2006.
- [155] A.S. Fabbicante, G.F. Ward, T.J. Fabbicante, Micro-denier nonwoven materials made using modular die units, U.S. Patent 6114017, 2000.
- [156] Z.Y. Tao, H. Xia, J. Cao, Q. Gao, *Malaria journal* 10 (2011) 251.
- [157] K. Singha, S. Maity, M. Singha, P. Paul, D.P. Gon, *International Journal of Textile Science* 1 (2012) 7.
- [158] W.E. Schortmann, Nonwoven laminate with wet-laid barrier fabric and related method, U.S. Patent 5204165, 1993.
- [159] Y. Tadokoro, M. Uesaka, Y. Takata, F. Goto, Wet-laid nonwoven fabric for battery separator, its production method and sealed type secondary battery, U.S. Patent 5888916, 1999.
- [160] W. Yi, Z. Huaiyu, H. Jian, L. Yun, Z. Shushu, *Journal of Power Sources* 189 (2009) 616.
- [161] P. Kritzer, *Journal of Power Sources* 161 (2006) 1335.
- [162] M. Tanaka, N. Tokutake, Alkaline battery separator and process for producing the same, U.S. Patent 6030727, 2000.
- [163] T. Ashida, T. Tsukuda, Nonwoven fabric for separator of non-aqueous electrolyte battery and non-aqueous electrolyte battery using the same, U.S. Patent 6200706, 2001.
- [164] A. Mathur, Recyclable thermoplastic moldable nonwoven liner for office partition and method for its manufacture, U.S. Patent 6517676, 2003.

- [165] J.R. Kim, S.W. Choi, S.M. Jo, W.S. Lee, B.C. Kim, *Electrochimica Acta* 50 (2004) 69.
- [166] S.W. Choi, S.M. Jo, W.S. Lee, Y.R. Kim, *Advanced Materials* 15 (2003) 2027.
- [167] K. Gao, X. Hu, C. Dai, T. Yi, *Materials Science and Engineering B* 131 (2006) 100.
- [168] S.S. Choi, Y.S. Lee, C.W. Joo, S.G. Lee, J.K. Park, K.S. Han, *Electrochimica Acta* 50 (2004) 339.
- [169] S.W. Lee, S.W. Choi, S.M. Jo, B.D. Chin, D.Y. Kim, K.Y. Lee, *Journal of Power Sources* 163 (2006) 41.
- [170] K. Hwang, B. Kwon, H. Byun, *Journal of Membrane Science* 378 (2011) 111.
- [171] C. Cao, L. Tan, W. Liu, J. Ma, L. Li, *Journal of Power Sources* 248 (2014) 224.
- [172] Y. Liang, S. Cheng, J. Zhao, C. Zhang, S. Sun, N. Zhou, Y. Qiu, X. Zhang, *Journal of Power Sources* 240 (2013) 204.
- [173] C. Yang, Z. Jia, Z. Guan, L. Wang, *Journal of Power Sources* 189 (2009) 716.
- [174] X. Li, G. Cheruvally, J.K. Kim, J.W. Choi, J.H. Ahn, K.W. Kim, H.J. Ahn, *Journal of Power Sources* 167 (2007) 491.
- [175] G. Cheruvally, J.K. Kim, J.W. Choi, J.H. Ahn, Y.J. Shin, J. Manuel, P. Raghavan, K.W. Kim, H.J. Ahn, D.S. Choi, C.E. Song, *Journal of Power Sources* 172 (2007) 863.
- [176] M.A. Kader, S.K. Kwak, S.L. Kang, J.H. Ahn, C. Nah, *Polymer International* 57 (2008) 1199.
- [177] M. Xiong, H. Tang, Y. Wang, Y. Lin, M. Sun, Z. Yin, M. Pan, *Journal of Power Sources* 241 (2013) 203.

- [178] P. Raghavan, J. Manuel, X. Zhao, D.S. Kim, J.H. Ahn, C. Nah, *Journal of Power Sources* 196 (2011) 6742.
- [179] P. Carol, P. Ramakrishnan, B. John, G. Cheruvally, *Journal of Power Sources* 196 (2011) 10156.
- [180] T.H. Cho, T. Sakai, S. Tanase, K. Kimura, Y. Kondo, T. Tarao, M. Tanaka, *Electrochemical and Solid-State Letters* 10 (2007) A159.
- [181] S.W. Choi, J.R. Kim, S.M. Jo, W.S. Lee, Y.R. Kim, *Journal of The Electrochemical Society* 152 (2005) A989.
- [182] T.H. Cho, M. Tanaka, H. Onishi, Y. Kondo, T. Nakamura, H. Yamazaki, S. Tanase, T. Sakai, *Journal of Power Sources* 181 (2008) 155.
- [183] M. Rao, X. Geng, Y. Liao, S. Hu, W. Li, *Journal of Membrane Science* 399–400 (2012) 37.
- [184] D. Bansal, B. Meyer, M. Salomon, *Journal of Power Sources* 178 (2008) 848.
- [185] Y. Ding, P. Zhang, Z. Long, Y. Jiang, F. Xu, W. Di, *Journal of Membrane Science* 329 (2009) 56.
- [186] P. Raghavan, X. Zhao, C. Shin, D.H. Baek, J.W. Choi, J. Manuel, M.Y. Heo, J.H. Ahn, C.W. Nah, *Journal of Power Sources* 195 (2010) 6088.
- [187] W. Jiang, Z. Liu, Q. Kong, J. Yao, C. Zhang, P. Han, G. Cui, *Solid State Ionics* 232 (2013) 44.
- [188] X. Zhou, L. Yue, J. Zhang, Q. Kong, Z. Liu, J. Yao, G. Cui, *Journal of the Electrochemistry Society* 160 (2013) A1341.
- [189] J. Hao, G. Lei, Z. Li, L. Wu, L. Wang, *Journal of Membrane Science* 428 (2013) 11.

- [190] C. J. Orendorff, T. N. Lambert, C. A. Chavez, M. Bencomo, K. R. Fenton, *Advanced Energy Materials* 3 (2013) 314.
- [191] W. Qi, C. Lu, P. Chen, L. Han, Q. Yu, R. Xu, *Materials Letters* 66 (2012) 239.
- [192] C. Lu, W. Qi, L. Li, J. Xu, P. Chen, R. Xu, L. Han, Q. Yu, *Journal of Applied Electrochemistry* 43 (2013) 711.
- [193] J. Zhang, Z. Liu, Q. Kong, C. Zhang, S. Pang, L. Yue, X. Wang, J. Yao, G. Cui, *ACS Applied Materials and Interfaces* 1 (2013) 128.
- [194] Q. Xu, Q. Kong, Z. Liu, X. Wang, R. Liu, J. Zhang, L. Yue, Y. Duan, G. Cui *ACS Sustainable Chemistry and Engineering* 2 (2014) 194.
- [195] Q. Xu, Q. Kong, Z. Liu, J. Zhang, X. Wang, R. Liu, L. Yue, G. Cui, *RSC Advances* 4 (2014) 7845.
- [196] J.P. Locquet, J. Perret, J. Fompeyrine, E. Machler, J.W. Seo, G. Van Tendeloo, *Nature* 394 (1998) 453.
- [197] F. Croce, R. Curini, A. Martinelli, L. Persi, F. Ronci, B. Scrosati, R. Caminiti, *The Journal of Physical Chemistry B* 103 (1999) 10632.
- [198] M. Kinouchi, T. Akazawa, T. Oe, R. Kogure, K. Kawabata, Y. Nakakita, Battery separator and lithium secondary battery, U.S. Patent 6627346, 2003.
- [199] Y.H. Liao, X.P. Li, C.H. Fu, R. Xu, L. Zhou, C.L. Tan, S.J. Hu, W.S. Li, *Journal of Power Sources* 196 (2011) 2115.
- [200] C.M. Yang, H.S. Kim, B.K. Na, K.S. Kum, B.W. Cho, *Journal of Power Sources* 156 (2006) 574.

- [201] J.Y. Kim, S.K. Kim, S.J. Lee, S.Y. Lee, H.M. Lee, S. Ahn, *Electrochimica Acta* 50 (2004) 363.
- [202] S.M. Eo, E. Cha, D.W. Kim, *Journal of Power Sources* 189 (2009) 766.
- [203] J.A. Choi, S.H. Kim, D.W. Kim, *Journal of Power Sources* 195 (2010) 6192.
- [204] J.H. Park, J.H. Cho, W. Park, D. Ryoo, S.J. Yoon, J.H. Kim, Y.U. Jeong, S.Y. Lee, *Journal of Power Sources* 195 (2010) 8306.
- [205] H. S. Jeong, S. C. Hong, S. Y. Lee, *Journal of Membrane Science* 364 (2010) 177.
- [206] D. Fu, B. Luan, S. Argue, M. N. Bureau, I. J. Davidson, *Journal of Power Sources* 206 (2012) 325.
- [207] W. K. Shin, D. W. Kim, *Journal of Power Sources* 226 (2013) 54.
- [208] K. Prasanna, C. S. Kim, C. W. Lee, *Materials Chemistry and Physics* 146 (2014) 545.
- [209] M. Kim, Y. C. Nho, J. H. Park, *Journal of Solid State Electrochemistry* 14 (2010) 769.
- [210] M. Kim, G.Y. Han, K.J. Yoon, J.H. Park, *Journal of Power Sources* 195 (2010) 8302.
- [211] H.S. Jeong, S.Y. Lee, *Journal of Power Sources* 196 (2011) 6716.
- [212] M. Kim, J. H. Park, *Journal of Power Sources* 212 (2012) 22.
- [213] J. Fang, A. Kellarakis, Y. W. Lin, C. Y. Kang, M. H. Yang, C. L. Cheng, Y. Wang, E. P. Giannelis, L. D. Tsai, *Phys. Chem. Chem. Phys.* 13 (2011) 14457.
- [214] T.H. Cho, M. Tanaka, H. Onishi, Y. Kondo, T. Nakamura, H. Yamazaki, S. Tanase, T. Sakai, *Journal of The Electrochemical Society* 155 (2008) A699.
- [215] H.S. Jeong, D.W. Kim, Y.U. Jeong, S.Y. Lee, *Journal of Power Sources* 195 (2010) 6116.
- [216] P.P. Prosini, P. Villano, M. Carewska, *Electrochimica acta* 48 (2002) 227.

- [217] D.W. Kim, *Journal of Power Sources* 87 (2000) 78.
- [218] N.S. Choi, J.K. Park, *Electrochimica Acta* 46 (2001) 1453.
- [219] M. Walkowiak, A. Zalewska, T. Jesionowski, M. Pokora, *Journal of Power Sources* 173 (2007) 721.
- [220] Y.T. Chen, Y.C. Chuang, J.H. Su, H.C. Yu, Y.W. Chen-Yang, *Journal of Power Sources* 196 (2011) 2802.
- [221] A. Du Pasquier, P.C. Warren, D. Culver, A.S. Gozdz, G.G. Amatucci, J.M. Tarascon, *Solid State Ionics* 135 (2000) 249.
- [222] K.M. Kim, N.G. Park, K.S. Ryu, S.H. Chang, *Electrochimica Acta* 51 (2006) 5636.
- [223] R. Miao, B. Liu, Z. Zhu, Y. Liu, J. Li, X. Wang, Q. Li, *Journal of Power Sources* 184 (2008) 420.
- [224] A. Subramania, N.T. Kalyana Sundaram, A.R. Sathiya Priya, G. Vijaya Kumar, *Journal of Membrane Science* 294 (2007) 8.
- [225] D. Takemura, S. Aihara, K. Hamano, M. Kise, T. Nishimura, H. Urushibata, H. Yoshiyasu, *Journal of Power Sources* 146 (2005) 779.
- [226] Z. Li, G. Su, X. Wang, D. Gao, *Solid State Ionics* 176 (2005) 1903.
- [227] H. Huang, S.L. Wunder, *Journal of Power Sources* 97-98 (2001) 649.
- [228] N.T. Kalyana Sundaram, A. Subramania, *Electrochimica Acta* 52 (2007) 4987.
- [229] S. Zhang, K. Xu, T. Jow, *Journal of Power Sources* 140 (2005) 361.
- [230] S.S. Zhang, K. Xu, T.R. Jow, *Journal of Solid State Electrochemistry* 7 (2003) 492.
- [231] Y. Ding, P. Zhang, Z. Long, Y. Jiang, F. Xu, W. Di, *Science and Technology of Advanced Materials* 9 (2008) 015005.

- [232] P. Raghavan, J.W. Choi, J.H. Ahn, G. Cheruvally, G.S. Chauhan, H.J. Ahn, C. Nah, *Journal of Power Sources* 184 (2008) 437.
- [233] P. Raghavan, X. Zhao, J.K. Kim, J. Manuel, G.S. Chauhan, J.H. Ahn, C. Nah, *Electrochimica Acta* 54 (2008) 228.
- [234] P. Raghavan, X. Zhao, J. Manuel, G.S. Chauhan, J.H. Ahn, H.S. Ryu, H.J. Ahn, K.W. Kim, C. Nah, *Electrochimica Acta* 55 (2010) 1347.
- [235] J.K. Kim, G. Cheruvally, X. Li, J.H. Ahn, K.W. Kim, H.J. Ahn, *Journal of Power Sources* 178 (2008) 815.
- [236] F. Zhang, X. Ma, C. Cao, J. Li, Y. Zhu, *Journal of Power Sources* 251 (2014) 423.
- [237] M. Yanilmaz, C. Chen, X. Zhang, *Journal of Polymer Science, Part B: Polymer Physics* 51 (2013) 1719.
- [238] M. Yanilmaz, Y. Lu, M. Dirican, K. Fu, X. Zhang, *Journal of Membrane Science* 456 (2014) 57.
- [239] H.R. Jung, D.H. Ju, W.J. Lee, X. Zhang, R. Kotek, *Electrochimica Acta* 54 (2009) 3630.
- [240] Y. Liang, L. Ji, B. Guo, Z. Lin, Y. Yao, Y. Li, M. Alcoutlabi, Y. Qiu, X. Zhang, *Journal of Power Sources* 196 (2011) 436.
- [241] T.H. Cho, M. Tanaka, H. Ohnishi, Y. Kondo, M. Yoshikazu, T. Nakamura, T. Sakai, *Journal of Power Sources* 195 (2010) 4272.
- [242] Y.S. Lee, Y.B. Jeong, D.W. Kim, *Journal of Power Sources* 195 (2010) 6197.
- [243] M. Yanilmaz, M. Dirican, X. Zhang, *Electrochimica Acta* 133 (2014) 501.

- [244] J. Zhang, L. Yue, Q. Kong, Z.Liu, X. Zhou, C. Zhang, S. Pang, X. Wang, J.Yao, G. Cui, *Journal of the Electrochemistry Society* 160 (2013) A769.
- [245] E. S.Choi, S. Y. Lee, *Journal of Materials Chemistry* 21 (2011) 14747.
- [246] H. S. Jeong, E. S.Choi, S. Y. Lee, *Electrochimica Acta* 86 (2012) 317.
- [247] C. Cao, Z. B. Li , X. L. Wang, X. B. Zhao, W. Q. Han, *Frontiers in EnergyResearch - EnergyStorage* (2014) doi: 10.3389/fenrg.2014.00025.
- [248] H. Kim, Y. Ding, P. A. Kohl, *Journal of Power Sources* 198 (2012) 281.
- [249] T. Inada, T. Kobayashi, N. Sonoyama, A.Yamada, S. Kondo, M. Nagao, R. Kanno, *Journal of Power Sources* 194 (2009) 1085.
- [250] V. Thangadurai, W. Weppner, *Journal of the American Ceramic Society* 88 (2005) 411.
- [251] O. Bohnke, *Solid State Ionics* 179 (2008) 9.
- [252] X. Xu, Z. Wen, J. Wu, X. Yang, *Solid State Ionics* 178 (2007) 29.
- [253] X. Xu, Z. Wen, Z. Gu, X. Xu, Z.Lin, *Chemistry Letters* 34 (2005).
- [254] K. Minami, A. Hayashi, and M. Tatsumisagow *Journal of the American Ceramic Society* 94 (2011) 1779.
- [255] R. Murugan, V. Thangadurai, W. Weppner, *Applied Physics A* 91 (2008) 615.
- [256] K. Dokko, N. Akutagawa, Y. Isshiki, K. Hoshina, K. Kanamura, *Solid State Ionics* 176 (2005) 2345.
- [257] A.M. Sukeshini , A.R. Kulkarni, A. Sharma, *Solid State Ionics* 113–115 (1998) 179.
- [258] L. Wang, N. Li, X. He, C. Wan, C. Jiang, *Electrochimica Acta* 68 (2012) 214.
- [259] J. Ji, J. Keen, W. H. Zhong, *Journal of Power Sources* 196 (2011) 10163.

- [260] P. Gavelin, R. Ljungback, P. Jannasch, B. Wesslen, *Solid State Ionics* 147 (2002) 325.
- [261] A. Chakrabarti, A. Juilfs, R. Filler, B. K. Mandal, *Solid State Ionics* 181 (2010) 982.
- [262] I. Basumallick, P. Roy, A. Chatterjee, A. Bhattacharya, S. Chatterjee, S. Ghosh, *Journal of Power Sources* 162 (2006) 797.
- [263] S.S Sekhon, H. Pal Singh, *Solid State Ionics* 152–153 (2002) 169–174.
- [264] S. W. Choi, J. R. Kim, S. M. Jo, W. S. Lee, Y.-R. Kim, *Journal of the Electrochemistry Society* 152 (2005) A989.
- [265] J Saunier, F Alloin, J.Y Sanchez, G Caillon, *Journal of Power Sources* 119–121, (2003) 454.
- [266] F. Croce, M. L. Focarete, . Hassoun, I. Meschinia, B. Scrosati, *Energy and Environmental Science* 4 (2011) 921.
- [267] J. R. Kim, S. W. Choi, S. M. Jo, W. S. Lee, B. C. Kim, *Journal of the Electrochemistry Society* 152 (2005) A295.
- [268] J. R. Kim, S. W. Choi, S. M. Jo, W. S. Lee, B. C. Kim, *Electrochimica Acta* 50 (2004) 69.
- [269] J. Cao, L. Wang, M. Fang, Y. Shang, L. Deng, J. Yang, J. Lia, H. Chen, X. He *Electrochimica Acta* 114 (2013) 527.
- [270] M. Rao, X. Geng, Y. Liao, S. Hu, W. Li, *Journal of Membrane Science* 399–400 (2012) 37.
- [271] X. Helan Flora, M. Ulaganathan, R.S. Babu, S. Rajendran, *Ionics* 18 (2012) 731.
- [272] A. Subramania, N.T.Kalyana Sundaram, G.Vijaya Kumar, *Journal of Power Sources* 153 (2006) 177.

- [273] A. I. Gopalan, P. Santhosh, K. M. Manesh, J. H. Nho, S. H. Kim, C. G. Hwang, K. P. Lee, *Journal of Membrane Science* 325 (2008) 683.
- [274] L. Zhao, H. Zhang, X. Li, J. Zhao, C. Zhao, X. Yuan, *Journal of Applied Polymer Science* 111 (2009) 3104.
- [275] A. I. Gopalan, K. P. Lee, K. M. Manesh, P. Santhosh, *Journal of Membrane Science* 318 (2008) 422.
- [276] Z. Zhong, Q. Cao, B. Jing, X. Wang, X. Li, H. Deng, *Materials Science and Engineering: B* 177 (2012) 86.
- [277] H. Li, Y. M. Chen, X. T. Ma, J. L. Shi, B. K. Zhu, L. P. Zhu, *Journal of Membrane Science* 379 (2011) 397.
- [278] Q. Cheng, Z. Cui, J. Li, S. Qin, F. Yan, J. Li, *Journal of Power Sources* 266 (2014) 401.
- [279] J. K. Kim, G. Cheruvally, X. Li, J. H. Ahn, K. W. Kim, H. J. Ah, *Journal of Power Sources* 178 (2008) 815.
- [280] H.J Walls, J. Zhou, J. A. Yerian, P. S. Fedkiw, S. A. Khan, M. K. Stowe, G. L. Baker *Journal of Power Sources* 89 (2000) 156.
- [281] S. Ahmad, S. Ahmad, S.A. Agnihotry, *Journal of Power Sources* 140 (2005) 151.
- [282] S. Sun, C. Li, L. Zhang, H.L. Du, J.S. B. Gray, *European Polymer Journal* 42 (2006) 1643.
- [283] L. Persi, F. Croce, B. Scrosati, E. Plichta and M. A. Hendrickson, *Journal of the Electrochemistry Society* 149 (2002) A212.

- [284] K. M. Kim, N. G. Park, K. S. Ryu, S. H. Chang, *Electrochimica Acta*, 51 (2006) 5636.
- [285] R. Kumara, A. Subramania, N.T. Kalyana Sundaram, G. Vijaya Kumar, I. Baskaran, *Journal of Membrane Science* 300 (2007) 104.
- [286] Y.H. Liao, M.M. Rao, W.S. Lia, L.T. Yang, B.K. Zhu, R. Xu, C.H. Fu, *Journal of Membrane Science* 352 (2010) 95.
- [287] S. Liu, N. Imanishi, , T. Zhang, A. Hirano, Y. Takeda, O. Yamamoto, J. Yang, *Journal of Power Sources* 195 (2010) 6847.
- [288] C. C. Yang, Z. Y. Lian, S. J. Linb, J. Y. Shih, W. H. Chen, *Electrochimica Acta* 134 (2014) 258.
- [289] J. Cao, L. Wang, M. Fang, X. He, J. Li, J. Gao, L. Deng, J. Wang, H. Chen, *Journal of Power Sources* 246 (2014) 499.
- [290] J. Cao, L. Wang, Y. Shang, M. Fang, L. Deng, J. Gao, J. Li, H. Chen, X. He, *Electrochimica Acta* 111 (2013) 674.
- [291] J. Cao, L. Wang, X. He, M. Fang, J. Gao, J. Li, L. Deng, H. Chen, G. Tian, J.Wang, S. Fan, *Journal of Materials Chemistry A* 1 (2013) 5955.
- [292] G. Cheruvally, J. K. Kim, J. W. Choi, J. H. Ahn , Y. J. Shin, J. Manuela, P. Raghavan, K. W. Kim, H. J. Ahn, D. S. Choi, C. E. Song, *Journal of Power Sources* 172 (2007) 863.
- [293] Y. Liao, C. Sun, S. Hu, W.Li, *Electrochimica Acta* 89 (2013) 461.
- [294] W. Zhai, H. Zhu, L. Wang, X. Liu, H. Yang, *Electrochimica Acta* 133 (2014) 623.
- [295] Z. Cai, Y. Liu, S. Liu, L. Li, Y. Zhang, *Energy and Environmental Science* 5 (2012) 5690.

- [296] Y. Liu, Z. Cai, L. Tan, L. Li, Energy and Environmental Science 5 (2012) 9007.
- [297] Y. Liu, L. Tan, L.Li, Chemical Communication 48 (2012) 9858.

Table and Figure Captions

Table 1. General requirements for separators used in lithium-ion batteries.

Table 2. Summarization of monolayer membranes.

Table 3. Summarization of multilayer membranes.

Table 4. Summarization of modified microporous membrane separators.

Table 5. Summarization of non-woven mat separators by electrospinning method.

Table 6. Summarization of composite membrane separators.

Figure 1. Schematic illustration of a typical lithium-ion battery.

Figure 2. SEM images of microporous membrane separators made by (a) dry process and (b) wet process [6]. Reproduced with the permission.

Figure 3. Fabrication processes of microporous membranes: (a) dry and (b) wet processes.

Figure 4. SEM images of a polymer film (a) before and (b) after stretching [28]. Reproduced with the permission.

Figure 5. SEM images of microporous membrane separators prepared by wet process: (a) Celgard [41], (b) Tonen [6], (c) Asahi [41], and (d) Entek [6]. Reproduced with the permission.

Figure 6. SEM images of a microporous membrane separator by phase inversion: (a) top surface, and (b) bottom surface [46]. Reproduced with the permission.

Figure 7. Schematic for the preparation process of the multilayer membrane. Redrawn from Ref. [111].

Figure 8. SEM images of (a) surface and (b) cross-section of PAN nanoparticle-coated [123], and (c) surface and (d) cross-section of PMMA nanoparticle-coated [124] multilayer membranes. Reproduced with the permission.

Figure 9. Schematic of typical electrospinning set-up.

Figure 10. SEM images of electrospun PVDF nonwoven mats: (a) before and (b) after absorbing liquid electrolyte [165]. Reproduced with the permission.

Figure 11. SEM images of electrospun PVDF-co-HFP nonwoven mats: (a) before and (b) after absorbing liquid electrolyte [5]. Reproduced with the permission.

Figure 12. SEM images of electrospun PAN nanofiber mats: (a) pristine membrane, (b) after immersing in liquid electrolyte, and (c) after charge-discharge cycles [181]. Reproduced with the permission.

Figure 13. Schematic of electrospun trilayer non-woven mats. Redrawn from Ref. [186].

Figure 14. Schematic of trilayer composite membrane. Redrawn from Ref. [210].

Figure 15. SEM images of Al₂O₃ particle-coated PE composite membranes prepared by different concentrations of non-solvent: (a) 2 %, (b) 4%, (c) 6 %, and (d) 8 % [215]. Reproduced with the permission.

Figure 16. SEM images of SiO₂ particle-coated PE composite membranes with different SiO₂ particle size: (a) without particles, (b) with particles of 530 nm, and (c) with particles of 40 nm [211]. Reproduced with the permission.

Figure 17. Schematic of laminating process and the morphology of composite membrane. Redrawn from Ref. [241].

Figure 18. SEM images of (a) PE membrane and (b) Al₂O₃/PVDF-co-CTFE fiber-coated PE membrane [242]. Reproduced with the permission.

Table 1. General requirements for separators used in lithium-ion batteries.

Parameter	Requirement
Chemical and electrochemical stabilities	stable for a long period of time
Wettability	wet out quickly and completely
Mechanical property	> 1000 kg/cm (98.06 MPa)
Thickness	20 – 25 μm
Pore size	< 1 μm
Porosity	40-60%
Permeability (Gurley)	< 0.025 sec/ μm
Dimensional stability	no curl up and lay flat
Thermal stability	< 5% shrinkage after 60 min at 90 °C
Shutdown	effectively shut down the battery at elevated temperatures

Table 2. Summarization of monolayer membranes.

Materials	Solvents	Processing method	Membrane Thickness	Liquid Electrolyte*	Electrolyte Uptake	Ionic Conductivity	Performance	Ref.
PP, PE		Dry and wet processes	13-57 μm	LiPF ₆ -EC/DMC		$0.4 \times 10^{-3} - 2.1 \times 10^{-3}$ S/cm	Thin thickness, high porosity, and large pore size	[50]
PP, PE		Dry and wet processes	25-50 μm	LiAsF ₆ -Cyclic ester/ether			Preventing thermal runaway	[51]
PP, PE			25 μm	LiPF ₆ -EC/PC/DEC			Low shutdown temperature	[52]
PP, PE		Dry and wet processes	20-25 μm	LiPF ₆ -EC/PC/DEC				[53]
PE	Paraffin oil	Wet process	25 μm	LiPF ₆ -PC			High mechanical strength	[54]
PVDF	Acetone/Butanol	Phase inversion		LiPF ₆ -PC/EC/DMC		3.7×10^{-3} S/cm	Regular discharging capacity and good rate capability	[56]
PVDF	Acetone/Ethanol	Phase inversion	35-50 μm	LiPF ₆ -EC/DMC/DEC		$3.0 \times 10^{-3} - 5.0 \times 10^{-3}$ S/cm	Stable discharge curves and low temperature performances	[57]
PVDF	DMF, TEP, NMP/water	Phase inversion	120-220 μm	LiPF ₆ -EC/DEC, LiPF ₆ -TEGDME	152-400%	2.0×10^{-3} S/cm	Sponge-like and finger-like structure	[58]
PVDF	NMP	Phase inversion	35-70 μm	LiPF ₆ -EC/DMC		$0.7 \times 10^{-3} - 2.1 \times 10^{-3}$ S/cm	Good cycling ability and high capacity at high charge rate	[59]
PVDF	DBP, DEHP/Ethanol	Phase inversion	200 μm	LiPF ₆ -DMC/EMC/EC	185-230%	1.3×10^{-3} S/cm	Good reservation of liquid electrolyte and good electrochemical stability	[60]
PVDF	EC/PC	Casting method	100-200 μm	LiSO ₃ CF ₃ , LiN(SO ₂ CF ₃) ₂ , LiPF ₆ -EC/DMC/PC		$0.3 \times 10^{-3} - 2.2 \times 10^{-3}$ S/cm	Good Li/polymer electrolyte interfacial stability	[61]
PAN	DMF	Phase inversion	60-70 μm	LiClO ₄ -EC/DMC, LiPF ₆ -EC/DMC, and LiBF ₄ -EC/DMC		$2.5 \times 10^{-3} - 2.8 \times 10^{-3}$ S/cm	Good electrochemical stability	[63]
PAN	EC/PC	Casting method		LiClO ₄ , LiN(SO ₂ CF ₃) ₂ , or LiAsF ₆ -EC/PC or BL/EC		$2.0 \times 10^{-3} - 6.1 \times 10^{-3}$ S/cm	Good electrochemical stability and good lithium cyclability	[66]
PAN, PMMA	EC/PC	Casting method	50-100 μm	LiN(SO ₂ CF ₃) ₂ -EC/DMC or LiClO ₄ -EC/PC		$0.1 \times 10^{-3} - 1.9 \times 10^{-3}$ S/cm	Good electrochemical stability	[67]
PMMA	PC	Casting method		LiClO ₄ -PC		1.0×10^{-4} S/cm	Low the activation energy of conduction	[68]

PMMA/PE GMe Blend	Acetonitrile/ DCM	Casting method	130 μm			$6.0 \times 10^{-5} - 2.0 \times 10^{-4}$ S/cm	Fast ionic transport and insufficient cycle life	[69]
PMMA, PAN	PC/EC	Casting method		LiClO ₄ -PC/EC, LiAsF ₆ -PC/EC, LiN(CF ₃ SO ₂) ₂ -PC/EC		1.0×10^{-4} S/cm	Good electrochemical stability and better cycle life	[70]
PVDF, PVDF-HFP		Phase inversion	120-220 μm	LiPF ₆ -EC/DEC	Enhanced	7.2×10^{-3} S/cm	Better ion transport	[73]
PVDF-HFP	NMP/Acetonitrile	Phase inversion		LiClO ₄ -EC/PC, LiPF ₆ -EC/DEC		$3.1 \times 10^{-4} - 1.6 \times 10^{-3}$ S/cm	Good electrochemical stability and cyclability	[74]
PVDF-HFP	Acetonitrile	Phase inversion	140 μm	LiBF ₄ -EC/GLB	120 %	3.4×10^{-3} S/cm	High thermal resistance and low capacity fading	[75]
P(HEA-AN)	DMF	Phase inversion		LiPF ₆ -EC/DEC/DMC	56-79 %	$1.1 \times 10^{-3} - 3.7 \times 10^{-3}$ S/cm	Good electrochemical stability	[76]
PMMA-AN-VAc	DMF	Phase inversion		LiPF ₆ -EC/DEC/DMC		3.5×10^{-3} S/cm	Good thermal stability and high electrochemical stability	[77]
PAN-MMA	DMF	Phase inversion		LiPF ₆ -EC/DEC/DMC		1.6×10^{-3} S/cm	Good electrochemical stability and cyclic stability	[78]
PVDF-HFP/PAN Blend	DMF	Solvent evaporation	150-200 μm	LiPF ₆ -EC/DEC	Enhanced	$1.5 \times 10^{-3} - 2.0 \times 10^{-3}$ S/cm	Good electrochemical stability and High specific capacity	[79]
PAN/PVP Blend	DMSO	Phase inversion	250 μm				High water permeability	[80]
PVDF/PMMA Blend	THF	Solvent evaporation		LiClO ₄ -EC/PC		$0.4 \times 10^{-4} - 4.0 \times 10^{-4}$ S/cm	Good mechanical strength and high ion diffusion coefficient	[81]
PVDF/PMMA Blend	DMSO	Phase inversion				Enhanced	Enhanced tensile strength and good thermal resistance	[82]
PVC/PMMMA Blend	THF	Solvent evaporation	250-300 μm	LiCF ₃ SO ₃ -EC/PC		$7.8 \times 10^{-6} - 1.4 \times 10^{-3}$ S/cm	Improved mechanical properties and good ionic transport	[84]
PAN-BuA/PVC Blend	PC	Phase inversion	40-80 μm	LiPF ₆ -EC/DEC	380%	$1.5 \times 10^{-3} - 2.0 \times 10^{-3}$ S/cm	High mechanical strength and good electrochemical stability	[85]
PVDF-HFP/DH-4-CN Blend	DMF	Phase inversion		LiPF ₆ -EC/DMC	190-417%	4.4×10^{-3} S/cm	Improved thermal property and good electrochemical stability	[89]
PVDF-HFP/PAML	DMF	Solvent evaporation	50 μm	LiBF ₄ -EC/DMC	75%	2.6×10^{-3} S/cm	Low discharge capacity and good discharge capacity retention	[87]

PVDF- HFP/PEO- EC Blend	Acetone	Phase inversion	180-190 μm	$\text{LiCF}_3\text{SO}_3\text{-EC/PC}$	3.5×10^{-5} S/cm	Enhanced mechanical strength	[88]
PVDF- HFP/PVAc Blend	THF	Solvent evaporation	140 μm	$\text{LiClO}_4\text{-EC/PC}$	2.3×10^{-3} S/cm	Good thermal property and high electrochemical stability	[89]

* Liquid electrolyte was used during the measurements of electrolyte uptake, ionic conductivity, and electrochemical performance.

Table 3. Summarization of multilayer membranes.

Materials	Substrate	Thickness	Liquid Electrolyte*	Electrolyte Uptake	Ionic Conductivity	Electrochemical Performance	Ref.
PP	PE	254 μm				Enhanced thermal properties	[108]
PP	PE	12-38 μm				Enhanced puncture strength and thermal resistance	[109]
PP	PE	31 μm				Enhanced mechanical and thermal properties	[110]
PVDF	PET	33 μm	LiPF ₆ -EC/DEC/PC	290%	8.9×10^{-4} S/cm	Better capacity retention and good electrochemical stability	[111]
AN/MMA	PE	30-45 μm	LiClO ₄ -EC/DMC	85-91%	7.7×10^{-4} - 1.1×10^{-3} S/cm	Stable discharge capacity and excellent rate performance	[112]
PVDF	PE	37 μm	LiPF ₆ -EC/DEC/PC	302%	1.1×10^{-3} S/cm	High discharge capacity and better high rate performance	[113]
PVDF	PET	50 μm	LiBF ₄ -EC/PC		2.1×10^{-4} - 6.4×10^{-3} S/cm	Good electrochemical stability and good charge-discharge efficiency	[114]
PVDF-HFP	PET	75 μm	LiN(CF ₃ SO ₂) ₂ -EC/PC		1.2×10^{-3} S/cm	Good capacity retention and stable coulombic efficiency	[115]
PVDF-HFP/PEGDMA Blend	PE		LiClO ₄ -EC/DEC	180-280%	5.0×10^{-5} - 4.0×10^{-4} S/cm	Enhanced electrical and thermal properties	[116]
PVDF-HFP/PEGDMA Blend	PE		LiClO ₄ -EC/DEC	125%	3.8×10^{-4} S/cm	Improved ionic conductivity and thermal resistance	[117]
PVDF/PMMA/PEGDA Blend	PET	100 μm	LiPF ₆ -EC/DMC/EMC	1000%	4.5×10^{-3} S/cm	Good cycle performance and high rate capacity	[118]
P3BT	PP	27 μm	LiPF ₆ -EC/PC			High rate charge-discharge capability and stable overcharge cycling performance	[120]
P3DT	PP/PE/PP	22 μm	LiPF ₆ -EC/DMC/EMC			Normal charge-discharge performance and good overcharging shutting capability	[121]
PTPAn	PP	27 μm	LiPF ₆ -EC/DMC/EMC			Good cycle performance and stable high rate performance with overcharging	[122]
PMMA	PE	25 μm	LiPF ₆ -EC/DEC	200%	5.2×10^{-4} S/cm	Better discharge C-rate performance	[124]
PAN	PET	40 μm	LiPF ₆ -EC/DMC/EMC	50-67%	9.8×10^{-5} - 6.7×10^{-4} S/cm	High specific capacity and good capacity retention	[123]
PVDF, PVDF-	PP	28-29 μm	LiPF ₆ -	90-130%		Better separator-electrode adhesion	[125]

CTFE			EC/DMC/EMC			
PVDF-HFP	PP	28-29 μm	LiPF ₆ - EC/DMC/EMC	90-130%	Stronger adhesion strength with electrode	[126]
PVDF	PMMA	75 μm	LiPF ₆ - EC/DMC/EMC	Enhanced	High discharge capacity and low capacity fading	[127]

* Liquid electrolyte was used during the measurements of electrolyte uptake, ionic conductivity, and electrochemical performance.

Table 4. Summarization of modified microporous membrane separators.

Substrate material	Modifying method	Induced materials	Membrane Thickness	Liquid Electrolyte*	Electrolyte Uptake	Ionic Conductivity	Performance	Ref.
PE	Plasma	AN	23 μm	LiPF ₆ -DEC/EMC/EC		1.4×10^{-3} S/cm	Good wettability, stable columbic efficiency and better cycle performance	[134]
PP	Electron beam	AA, DEGDM	50 μm	LiAsF ₆ -PC/EC/DME		1.0×10^{-3} S/cm	Good mechanical and wettability	[135]
PE	Electron beam	GMA		LiPF ₆ -DMC/EC			Less electrolyte leakage and better cycle life	[136]
PE	Electron beam	MMA	28-42 μm	LiPF ₆ -DMC/EC	180-210%	0.9×10^{-3} - 1.0×10^{-3} S/cm	Stable cycle performance and excellent discharge capacity	[137]
PE	Electron beam	PEGBA	20 μm	LiPF ₆ -DMC/EC		4.1×10^{-4} - 6.2×10^{-4} S/cm	Enhanced electrochemical stability and better cycle performance	[138]
PE	Electron beam	Siloxane	20 μm	LiPF ₆ -DMC/EC	180-200%	7.0×10^{-4} S/cm	Enhanced electrochemical stability and stable cycling performance	[139]
PE	Gamma ray	None		LiPF ₆ -EMC/EC		9.0×10^{-4} S/cm	Improved thermal resistance and good capacity retention	[140]
PVDF	Gamma ray	AA and DMAM	80-100 μm	LiPF ₆ -PC/EC	25-38%		Good rate performance and stable cycle behavior	[141]
PVDF	UV	TPGDA	90 μm	LiCF ₃ SO ₃ -TEGDME		8.0×10^{-4} - 1.6×10^{-3} S/cm	Better mechanical stability and improved cycling performance	[142]
PVDF-HFP	UV	PEGDA	50 μm	LiPF ₆ -DMC/EC		4.0×10^{-3} S/cm	Higher liquid electrolyte retention and better cycling performance and interfacial property	[143]
PE	coating	PDA	16 μm	LiPF ₆ -DEC/EC	169-202%	0.7 - 0.9×10^{-3} S/cm	Enhanced rate capability and cell performance	[144]
PE	coating	PDA		LiClO ₄ -EC/PC	112%	0.3×10^{-3} S/cm	Increased electrolyte uptake and improved cycling performance	[145]

PE	coating	PDA	25 μm	LiPF ₆ - DEC/EC/PC	126%	0.41×10^{-3} S/cm	Improved ionic conductivity and C-rate performance	[146]
PP	grafting	PEG		LiPF ₆ - DMC/EC/EMC		1.0×10^{-3} S/cm	Enhanced ionic conductivity, improved interfacial resistance and cycling performance	[147]
PE	coating	SiO ₂ -PDA			121%	0.35×10^{-3} S/cm	Increased wettability and improved C-rate performance	[148]
PP	dipping	PEO		LiPF ₆ - DMC/EC/EMC	149%	1.1×10^{-3} S/cm	Increased electrochemical stability and enhanced ionic conductivity	[149]
PE	coating	PI		LiPF ₆ EC/DEC	106%	2.4×10^{-4} S/cm	Improved thermal stability	[49]
PE	coating	PVDF- HFP/PMMA	22 μm	LiClO ₄ EC/DEC	403%	1.69×10^{-3} S/cm	Improvement in porosity, ionic conductivity, and cycling performance	[151]
PE	grafting	PDA/PMMA		LiPF ₆ EC/DMC/DEC	210%	1.2×10^{-3} S/cm	Improved electrolyte uptake and ionic conductivity and better cycle performance	[150]

* Liquid electrolyte was used during the measurements of electrolyte uptake, ionic conductivity, and electrochemical performance.

Table 5. Summarization of non-woven mat separators by electrospinning method.

Materials	Solvents	Membrane Thickness	Fiber Diameter	Liquid Electrolyte*	Electrolyte Uptake	Ionic Conductivity	Electrochemical Performance	Ref.
PVDF	Acetone/DMAc	30 μm	0.45 μm	LiPF ₆ -EC/DMC/DEC	320-350%	1.0×10^{-3} S/cm	Stable charge-discharge and good cycle performance	[165]
PVDF	Acetone/DMAc		0.25 μm	LiPF ₆ -EC/DMC	260%	1.7×10^{-3} S/cm	Good oxidation stability	[166]
PVDF	Acetone/DMF		0.51 – 0.88 μm	LiPF ₆ -EC/DMC			Stable charge-discharge and high discharge capacity	[167]
PVDF	DMAA	20 μm	0.40 μm	LiN(CF ₃ SO ₂) ₂		1.6×10^{-3} – 2.0×10^{-3} S/cm		[168]
PVDF/PVDF-co-HFP	Acetone/DMAc	17 μm	0.42 μm	LiPF ₆ -EC/DMC/DEC	280%	1.0×10^{-3} S/cm	Good cycle performance	[169]
PVDF	DMF	50 – 75 μm	0.10 – 0.13 μm				Excellent rate capability	[173]
PVDF-co-HFP	Acetone/DMAc	100 – 125 μm	0.6 – 1.5 μm	LiPF ₆ -EC/DMC LiCF ₃ SO ₃ -TEGDME	160-210%	0.4×10^{-3} S/cm	Good electrochemical stability and cycle performance	[174]
PVDF-co-HFP	Acetone/DMAc	80 μm	1.0 μm	LiTFSI-BMITFSI LiBF ₄ -BMIBF ₄	600-750%	2.3×10^{-3} S/cm	Stable cycle performance	[175]
PVDF-co-HFP	Acetone/DMAc	30 μm	0.5 – 2.3 μm	LiPF ₆ -EC/DMC/DEC	270-370%	1.0×10^{-3} S/cm	Good charge-discharge and little capacity fade	[5]
PVDF-g-tBA	Acetone/DMAc			LiCF ₃ SO ₃ -TEGDME		1.2×10^{-3} – 1.5×10^{-3} S/cm	Good electrochemical stability and improved cycle performance	[176]
PAN	DMF	100 μm	0.28 – 0.44 μm	LiPF ₆ -EC/DMC, EC/DEC, EC/EMC, PC	395-479%	2.0×10^{-3} – 2.14×10^{-3} S/cm	Good cycle performance and low capacity fade	[178]
PAN	DMF	250 μm	0.88 – 1.26 μm	LiPF ₆ -EC/DMC/DEC	1100%	1.7×10^{-5} S/cm	Stable charge-discharge capacity and good mechanical stability	[179]
PAN	DMF	33 – 35 μm	0.35 μm	LiPF ₆ -EC/DEC			Superior rate capability and small ionic resistance at high rate	[180]

PAN	DMF	30 μm	0.33 μm	LiPF ₆ -EC/DMC, EC/EMC, EC/DEC, EC/DMC/DEC		1.0×10^{-3} S/cm	High discharge capacity and stable cyclic performance	[181]
PAN	DMF	25 – 35 μm	0.25 – 0.38 μm	LiPF ₆ -EC/DEC		1.5×10^{-3} – 2.6×10^{-3} S/cm	Good cycle performance and high rate capability	[182]
PAN/PMMA Blend	DMF		0.45 μm	LiTFSI- PYR ₁₄ TFSI/PEGDME	480%	3.6×10^{-3} S/cm	Good electrochemical stability and stable cycle performance	[183]
PI/ PVDF- HFP and PI/ PAN Blend	NMP/DMC	25 μm	0.30 – 0.65 μm	LiPF ₆ -EC/EMC		0.15×10^{-3} – 1.5×10^{-3} S/cm	No capacity fade and good cycle performance	[184]
PVDF/PAN Blend	Acetone/DMF	45 μm	250 – 400 nm	LiClO ₄ -PC	250-300%	3.8×10^{-3} – 7.8×10^{-3} S/cm	Good anodic stability and higher electrochemical stability window	[71]
PVDF-co- HFP/PMMA Blend	Acetone/DMF	150 – 250 μm	200 – 350 nm	LiPF ₆ -EC/DMC	377%	1.99×10^{-3} S/cm	Stable discharge behavior and little capacity loss	[185]
PAN and PVDF-co- HFP	DMF	100 μm	320 – 490 nm	LiPF ₆ -EC/DMC	460-485%	3.9×10^{-3} – 6.5×10^{-3} S/cm	High electrochemical stability window and stable cycle performance with good discharge capacity	[186]

* Liquid electrolyte was used during the measurements of electrolyte uptake, ionic conductivity, and electrochemical performance.

Table 6. Summarization of composite membranes.

Substrate	Binder	Inorganic Particle	Membrane Thickness	Liquid Electrolyte*	Electrolyte Uptake	Ionic Conductivity	Electrochemical Performance	Ref.
PE, PP		SiO ₂ , MgO, ZrO ₂ , Al ₂ O ₃	25-26 μm	LiPF ₆ -DMC			Good discharge capacity retention	[198]
PP	PEO/PVDF-HFP	Al ₂ O ₃	26 μm	LiPF ₆ -EC/DMC/EMC	273%	3.8 × 10 ⁻³ S/cm	Good rate capacity and cycle stability	[199]
PP	PVDF/PEGDA/PMMA	BaTiO ₃ , TiO ₂ , Al ₂ O ₃	25 μm	LiPF ₆ /LiCF ₃ SO ₃ -EC/DMC/EMC		1.3 × 10 ⁻³ – 1.7 × 10 ⁻³ S/cm	Good interfacial stability and cycling performance	[200]
Polyolefin	PVDF-HFP	SiO ₂		LiPF ₆ -EC/PC/DEC	Enhanced	Enhanced	Excellent discharge performance	[201]
PE	PVDF-HFP	AlF ₃ , AlI ₃ , LiF, LiI	30 μm	LiClO ₄ -EC/DMC	Enhanced	0.8 × 10 ⁻³ – 1.2 × 10 ⁻³ S/cm	Good capacity retention and better high rate performance	[202]
PE	PLSS	Al ₂ O ₃	30 μm	LiPF ₆ -EC/DMC	206-248%	7.2 × 10 ⁻⁴ – 8.3 × 10 ⁻⁴ S/cm	Better capacity retention and cycling performance	[203]
PE	PMMA	SiO ₂	28 μm	LiPF ₆ -EC/DEC	Enhanced	7.4 × 10 ⁻⁴ S/cm	Improved discharge capacity and C-rate capability	[204]
PMMA	PVDF	Al ₂ O ₃	30 μm	LiPF ₆ -EC/DEC/EMC	~500%	5.3 × 10 ⁻⁴ S/cm	Good capacity retention and high electrochemical stability	[210]
PE	PVDF	SiO ₂	30 μm	LiPF ₆ -EC/DEC		0.53 – 0.61 S	Good discharge C-rate capability and better cycle performance	[211]
PP, PE	Roll-press	SiO ₂	28-44 μm	LiPF ₆ -EC/DEC	Enhanced	0.9 × 10 ⁻³ – 1.0 × 10 ⁻³ S/cm	Stable charge-discharge performance and high capacity retention	[214]
PE	PVDF-HFP	Al ₂ O ₃	30 μm	LiPF ₆ -EC/DEC		5.1 × 10 ⁻⁴ S/cm	Superior discharge C-rate capacity	[215]
PVDF-HFP		LiAlO ₂ , MgO, Al ₂ O ₃	30-50 μm	LiPF ₆ -EC/DMC		3.9 × 10 ⁻⁴ S/cm	Good electrochemical stability and better capacity retention	[216]
PE-MA		SiO ₂	40-60 μm	LiBF ₄ -EC/EMC/PC	Enhanced	5.8 × 10 ⁻⁴ S/cm	Good electrochemical stability and better charge-discharge performance	[217]
PVC/PMM A Blend		SiO ₂	45-50 μm	LiClO ₄ -EC/DMC	120-165%	1.1 × 10 ⁻³ S/cm	High discharge specific capacity and better cycle performance	[218]
PVDF-HFP		SiO ₂		LiPF ₆ -EC/DEC	Enhanced	Increased by 2 order	Good electrochemical stability	[219]

PAN	LiClO ₄ , SiO ₂	150 μm			of magnitude 1.4 × 10 ⁻⁴ – 6.0 × 10 ⁻⁴ S/cm	and stable cycle performance Better electrochemical stability and cyclability	[220]
PVDF-HFP	SiO ₂	50-75 μm	LiPF ₆ -EC/DMC	Enhanced	0.9 × 10 ⁻⁴ – 3.1 × 10 ⁻⁴ S/cm	Good discharge rate capability	[221]
PVDF-HFP	TiO ₂	80-100 μm	LiPF ₆ -EC/DMC	200-400%	Higher than 10 ⁻³ S/cm	Good electrochemical stability and low interfacial resistance	[222]
PVDF-HFP	TiO ₂	50 μm	LiPF ₆ -EC/DMC	360%	1.7 × 10 ⁻³ S/cm	Good interfacial stability and better rate capability	[223]
PVDF-HFP	ZrO ₂	50-80 μm	LiClO ₄ -EC/DEC	91%	1.1 × 10 ⁻² S/cm	Higher discharge capacity and lower capacity fading	[224]
PVDF	Al ₂ O ₃	20 μm	LiPF ₆ -EC/DEC			Excellent cycling performance and good thermal stability	[225]
PVDF-HFP	Al ₂ O ₃		LiClO ₄ -EC/DEC		0.8 × 10 ⁻³ – 2.1 × 10 ⁻³ S/cm	Good ion transport	[226]
PVDF- HFP/PS Blend	SiO ₂		LiPF ₆ - EC/DMC/DEC	Enhanced	4.0 × 10 ⁻³ S/cm	Increased pore volume and better ionic conductivity	[227]
PVDF- HFP/PVA Blend	LiAlO ₂	50-80 μm	LiClO ₄ -EC/DEC	120%	8.1 × 10 ⁻³ S/cm	Low interfacial resistance and good capacity retention	[228]
PTFE	CaCO ₃	175-190 μm	LiPF ₆ -EC/EMC	Enhanced	2.4 × 10 ⁻³ S/cm	Good high-rate performance and excellent capacity retention	[229]
PTFE	CaCO ₃		LiPF ₆ -EC/EMC	Enhanced	2.5 × 10 ⁻³ – 4.0 × 10 ⁻³ S/cm	Better cycling performance and good rate capability	[230]
PVDF	TiO ₂	30 μm	LiPF ₆ -EC/DMC	367%	1.4 × 10 ⁻³ S/cm	Good cycling performance and better capacity retention	[231]
PVDF-HFP	SiO ₂	150 μm	LiPF ₆ -EC/DMC	490-620%	5.1 × 10 ⁻³ – 8.1 × 10 ⁻³ S/cm	Better electrochemical stability and stable initial charge-discharge property	[232]
PVDF-HFP	BaTiO ₃ , Al ₂ O ₃ , SiO ₂	150 μm	LiPF ₆ -EC/DMC	459-462%	5.9 × 10 ⁻³ – 7.2 × 10 ⁻³ S/cm	Better discharge capacity and good cycle performance	[233]
PVDF-HFP	BaTiO ₃ , RTIL	150 μm	LiTFSI-BMITFSI	725-750%	3.6 × 10 ⁻³ – 5.2 × 10 ⁻³ S/cm	Good compatibility with electrode and better cycle performance	[234]
PVDF-HFP	SiO ₂	100-120 μm	LiTFSI-BMITFSI	400%	2.3 × 10 ⁻³ – 4.3 × 10 ⁻³	Enhanced charge-discharge	[235]

					S/cm	capacity and stable cycle performance	
PAN		SiO ₂		LiPF ₆ -EC/DMC	450-490%	1.1×10^{-2} S/cm	Better electrochemical stability and good cycle retention [239]
PAN		LLTO		LiPF ₆ -EC/EMC	480-510%	2.0×10^{-3} S/cm	higher electrochemical stability and stable cycle performance [240]
PE/PP	PAN	Al ₂ O ₃ , SiO ₂	34 μm	LiPF ₆ -EC/DEC			Better rate capability and stable cycle performance [241]
PVDF-CTFE		Al ₂ O ₃	25 μm	LiPF ₆ -EC/DEC	219%	5.7×10^{-4} S/cm	Good capacity retention and cycle performance [242]

* Liquid electrolyte was used during the measurements of electrolyte uptake, ionic conductivity, and electrochemical performance.

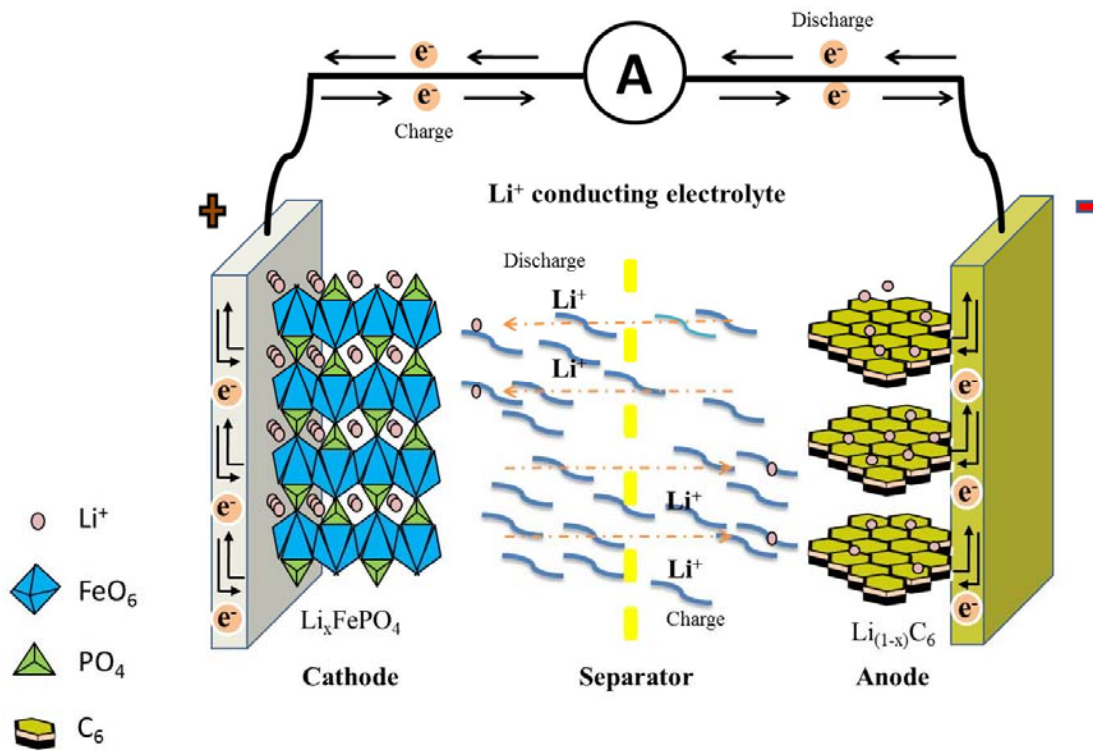


Figure 1. Schematic illustration of a typical lithium-ion battery.

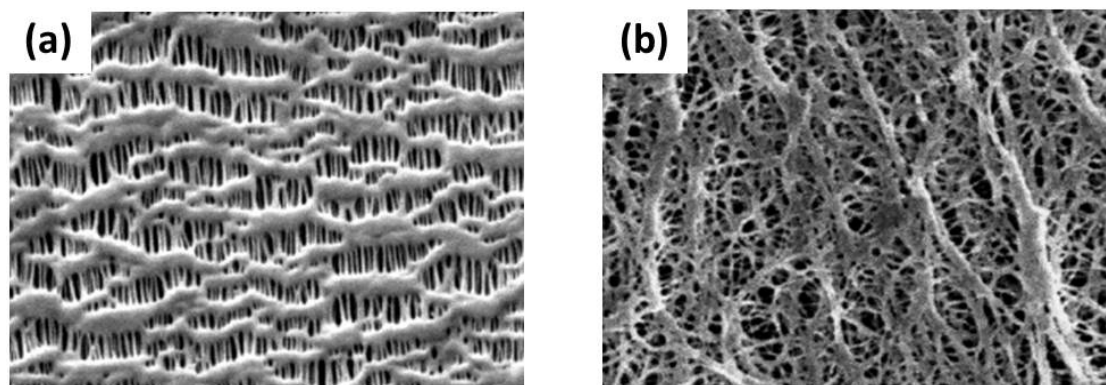


Figure 2. SEM images of microporous membrane separators made by (a) dry process and (b) wet process [6]. Reproduced with permission.

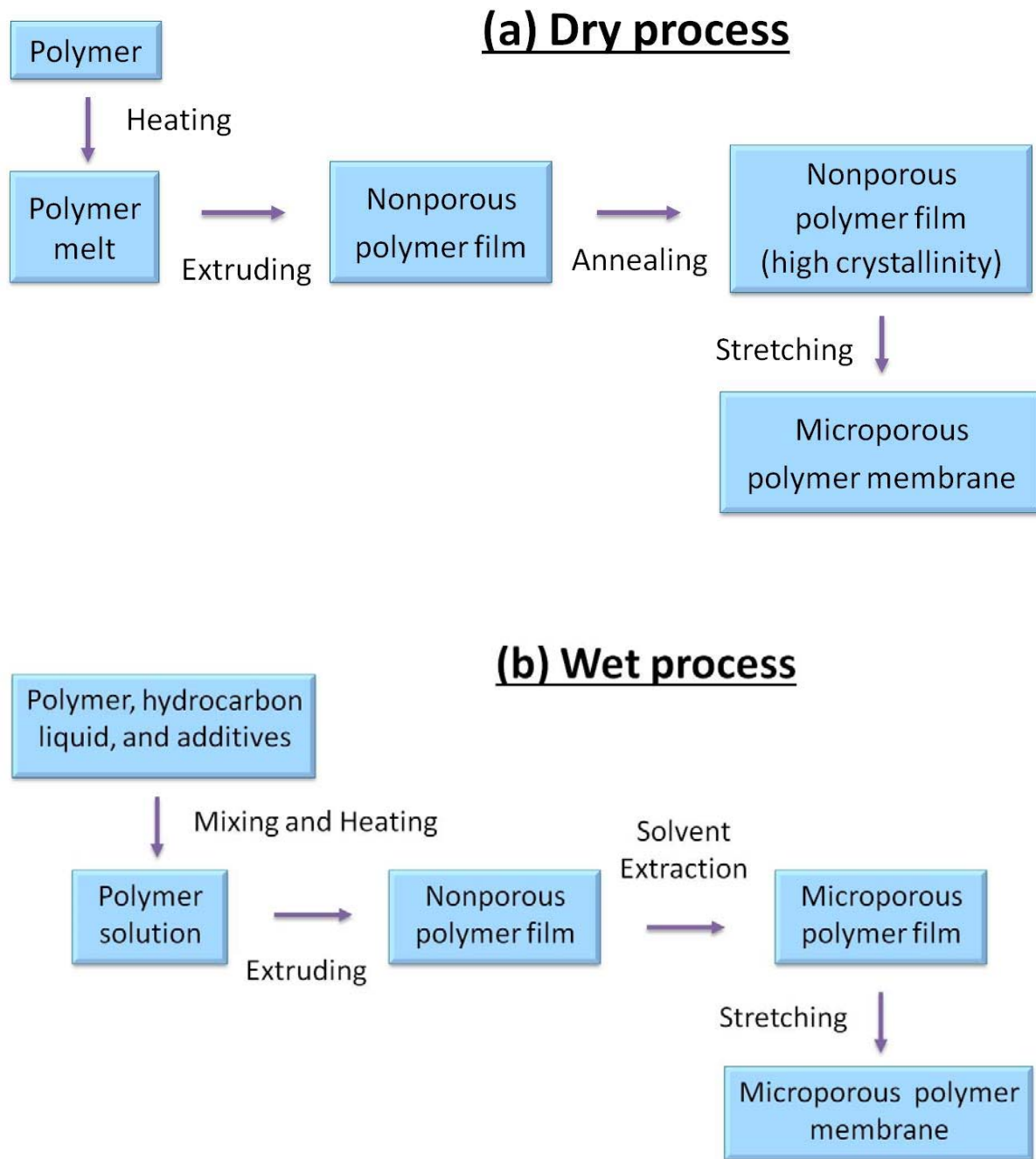


Figure 3. Fabrication processes of microporous membranes: (a) dry and (b) wet processes.

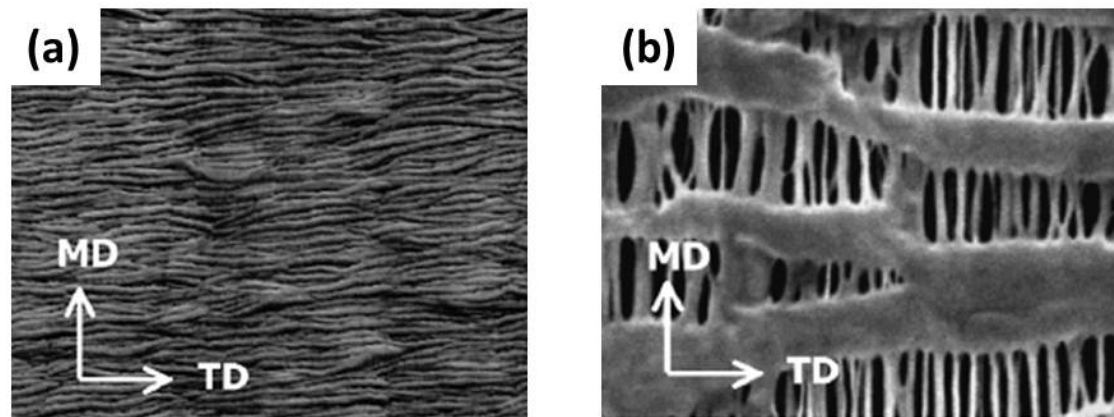


Figure 4. SEM images of a polymer film (a) before and (b) after stretching [28]. Reproduced with the permission.

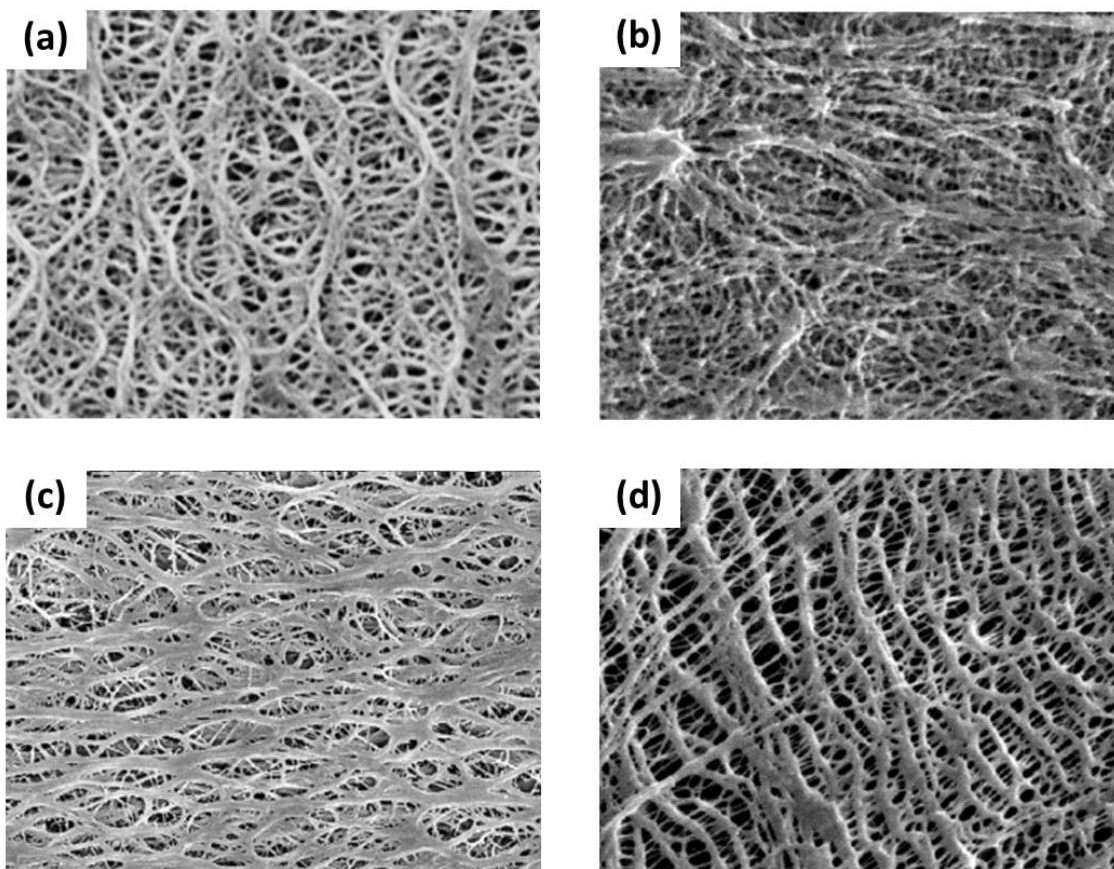


Figure 5. SEM images of microporous membrane separators prepared by wet process: (a) Celgard [41], (b) Tonen [6], (c) Asahi [41], and (d) Entek [6]. Reproduced with the permission.

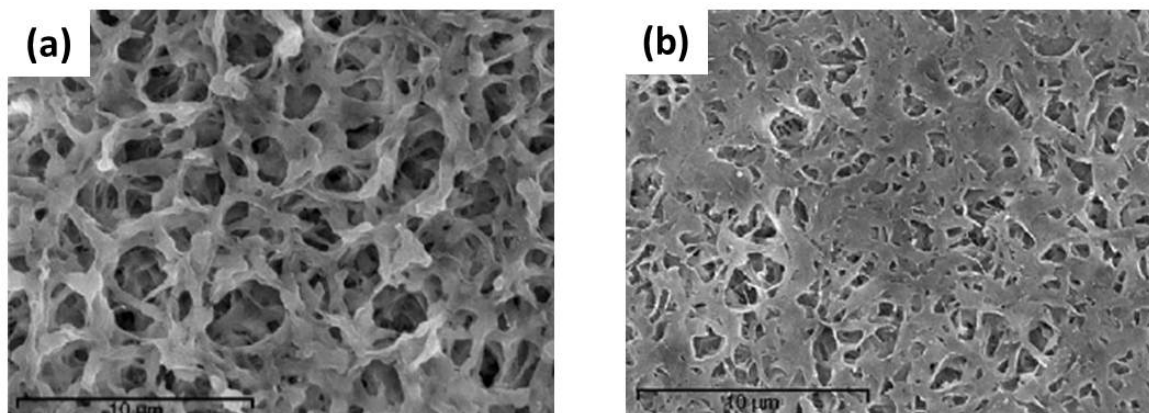


Figure 6. SEM images of a microporous membrane separator by phase inversion: (a) top surface, and (b) bottom surface [46]. Reproduced with the permission.

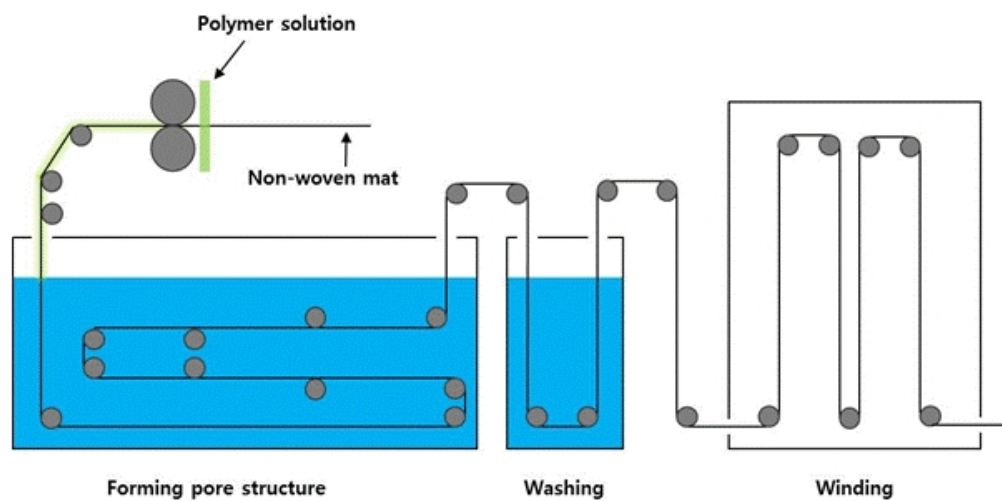


Figure 7. Schematic for the preparation process of the multilayer membrane. Redrawn from Ref. [111].

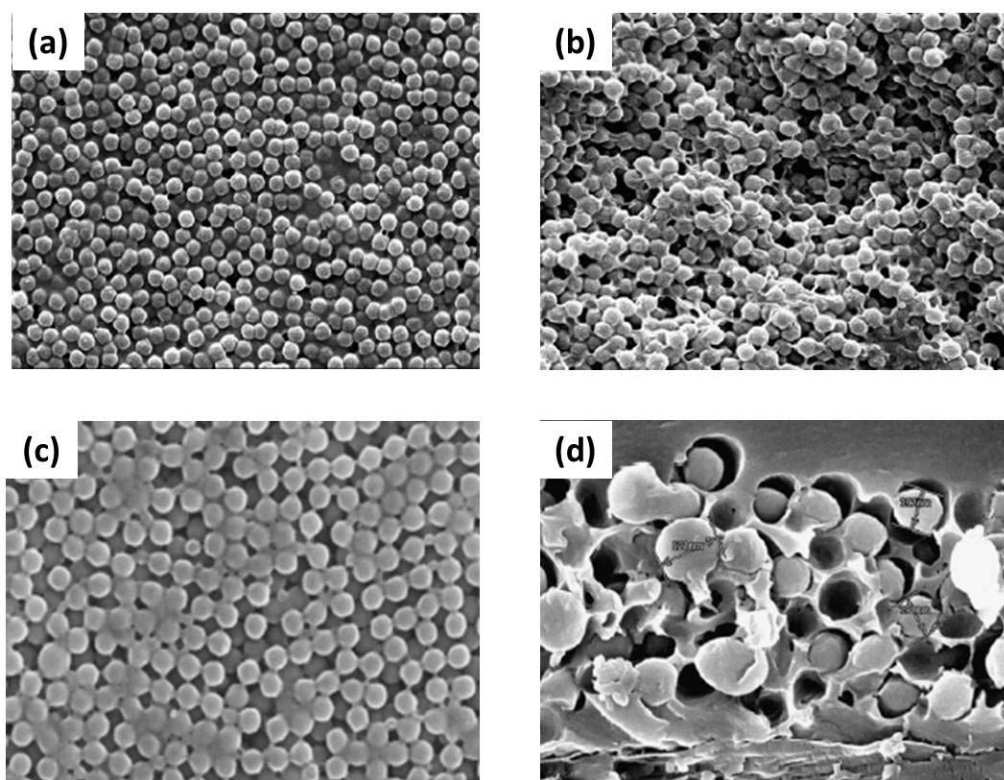


Figure 8. SEM images of (a) surface and (b) cross-section of PAN nanoparticle-coated [123], and surface (c) and (d) cross-section of PMMA nanoparticle-coated [124] multilayer membranes. Reproduced with the permission.

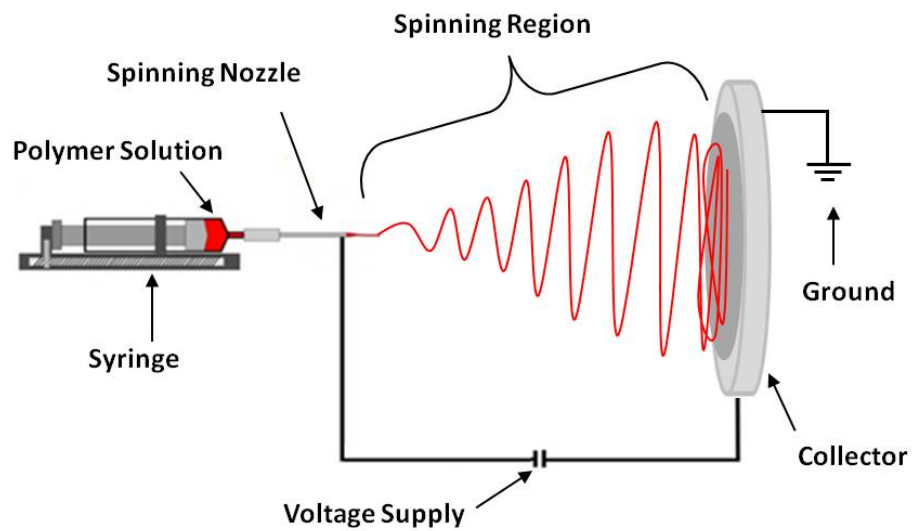


Figure 9. Schematic of typical electrospinning set-up

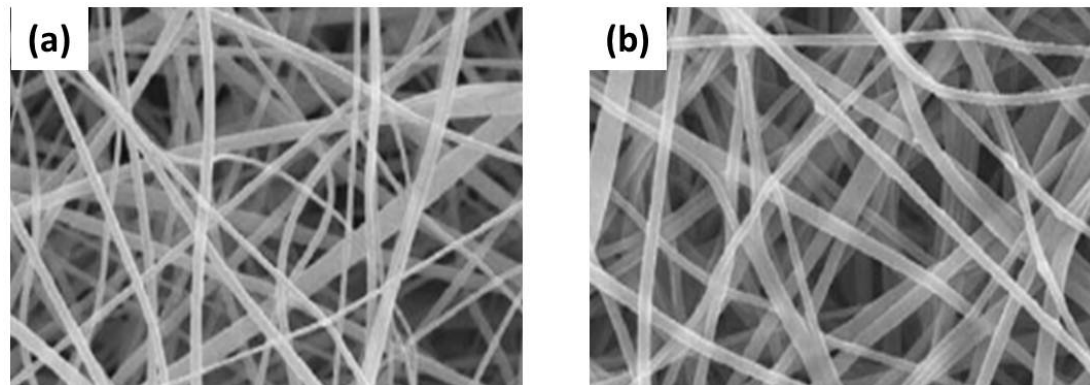


Figure 10. SEM images of electrospun PVDF nonwoven mats: (a) before and (b) after absorbing liquid electrolyte [165]. Reproduced with the permission.

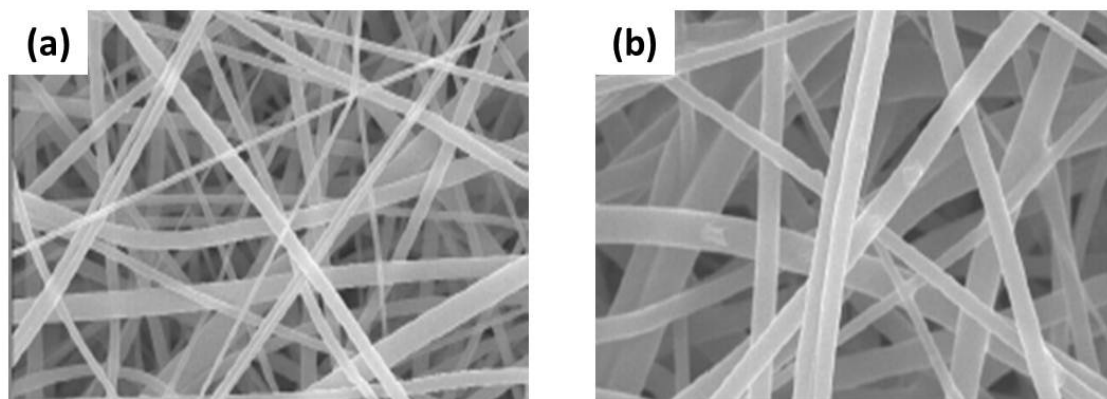


Figure 11. SEM images of electrospun PVDF-co-HFP nonwoven mats: (a) before and (b) after absorbing liquid electrolyte [5]. Reproduced with the permission.

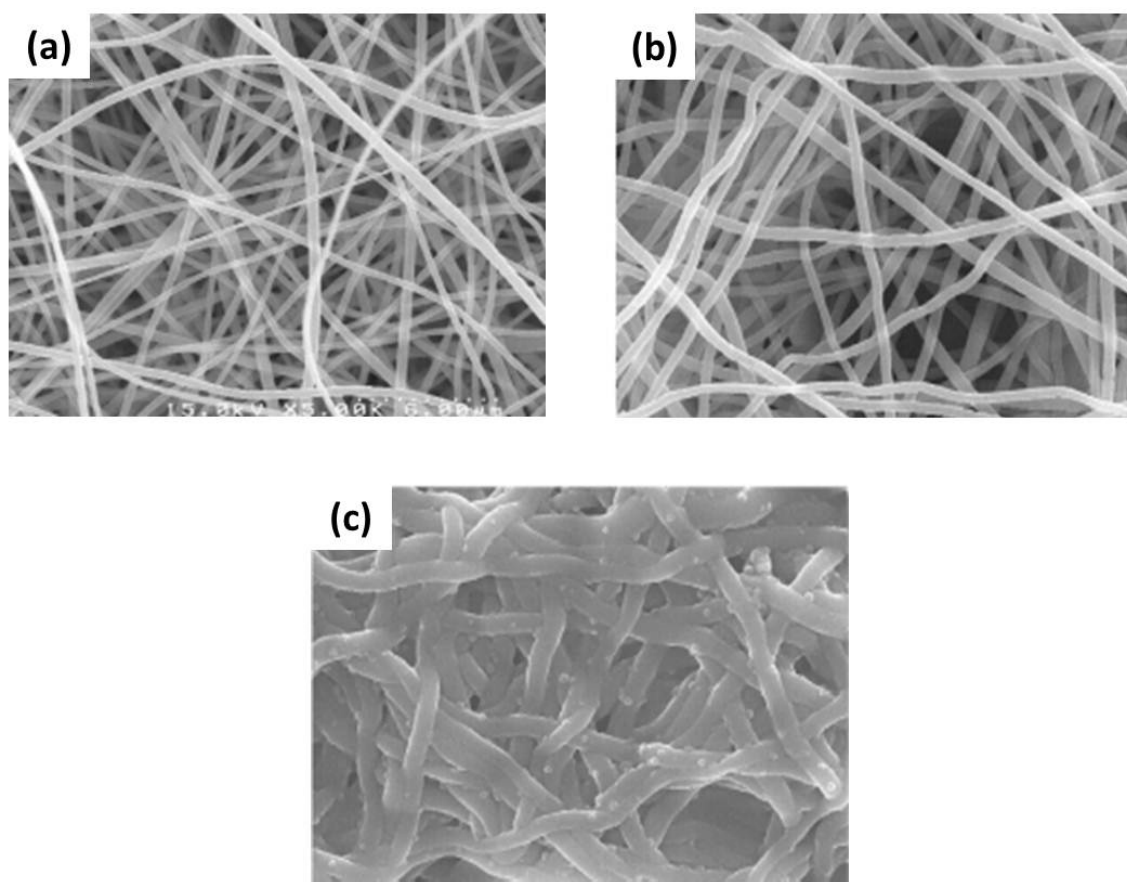


Figure 12. SEM images of electrospun PAN nanofiber mats: (a) pristine membrane, (b) after immersing in liquid electrolyte, and (c) after charge-discharge cycles [181]. Reproduced with the permission.

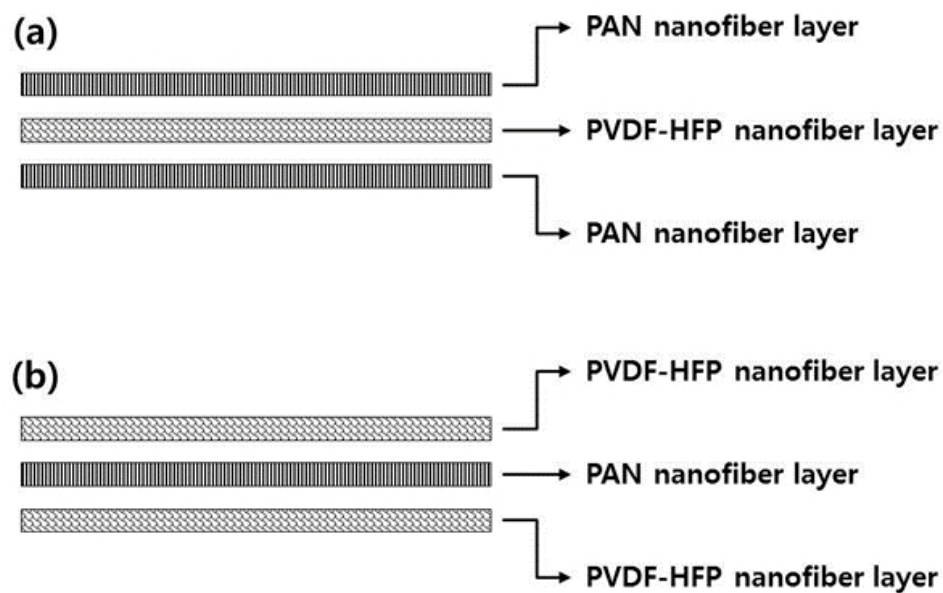


Figure 13. Schematic of electrospun trilayer non-woven mats. Redrawn from Ref. [186].

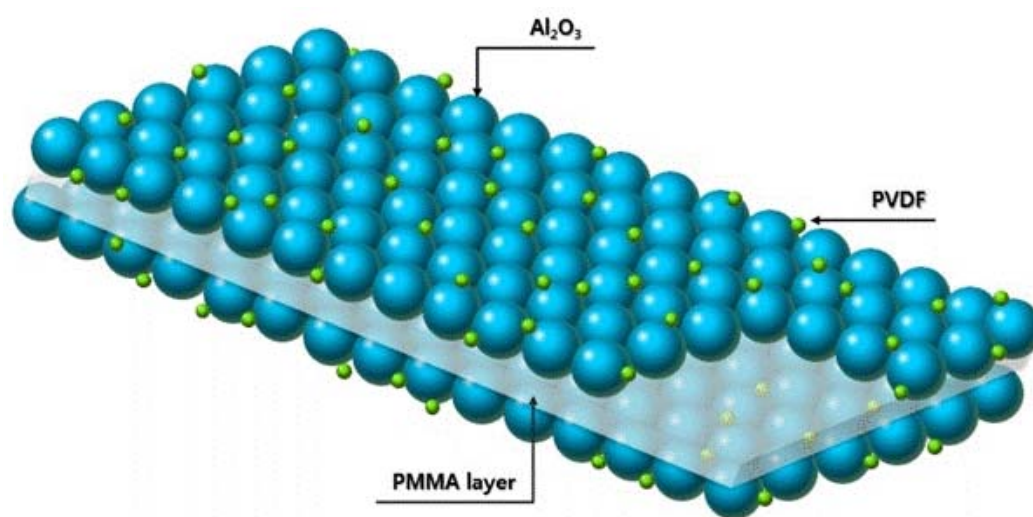


Figure 14. Schematic of trilayer composite membrane. Redrawn from Ref. [210].

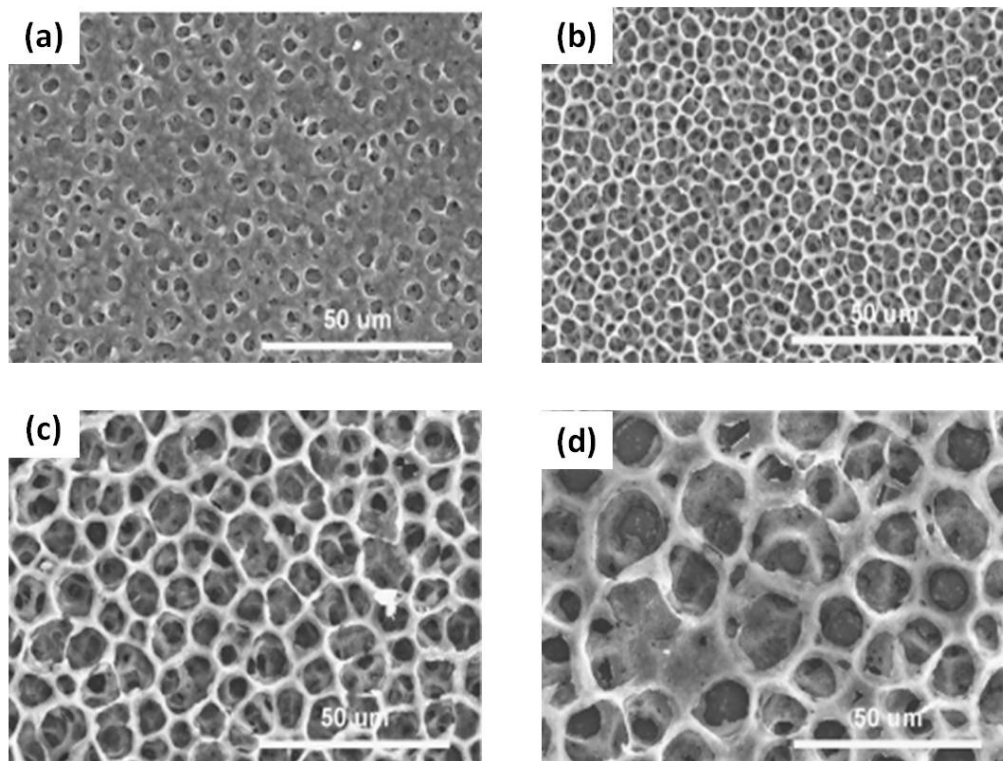


Figure 15. SEM images of Al_2O_3 particle-coated PE composite membranes prepared by different concentrations of non-solvent: (a) 2 %, (b) 4%, (c) 6 %, and (d) 8 % [215].

Reproduced with the permission.

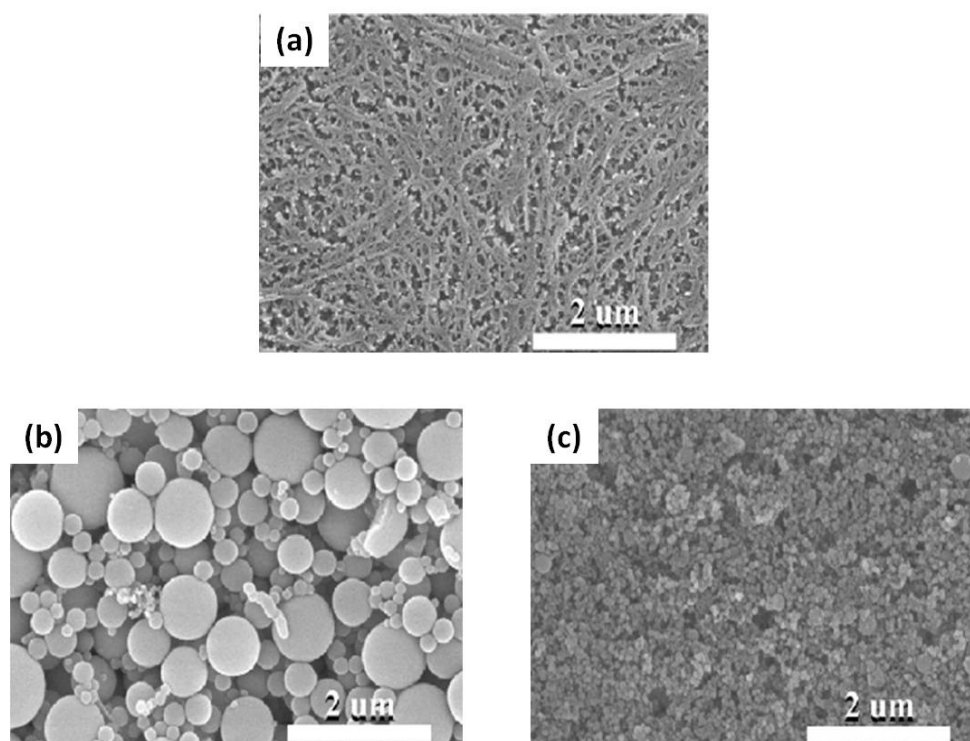


Figure 16. SEM images of SiO₂ particle-coated PE composite membranes with different SiO₂ particle size: (a) without particles, (b) with particles of 530 nm, and (c) with particles of 40 nm [211]. Reproduced with the permission.

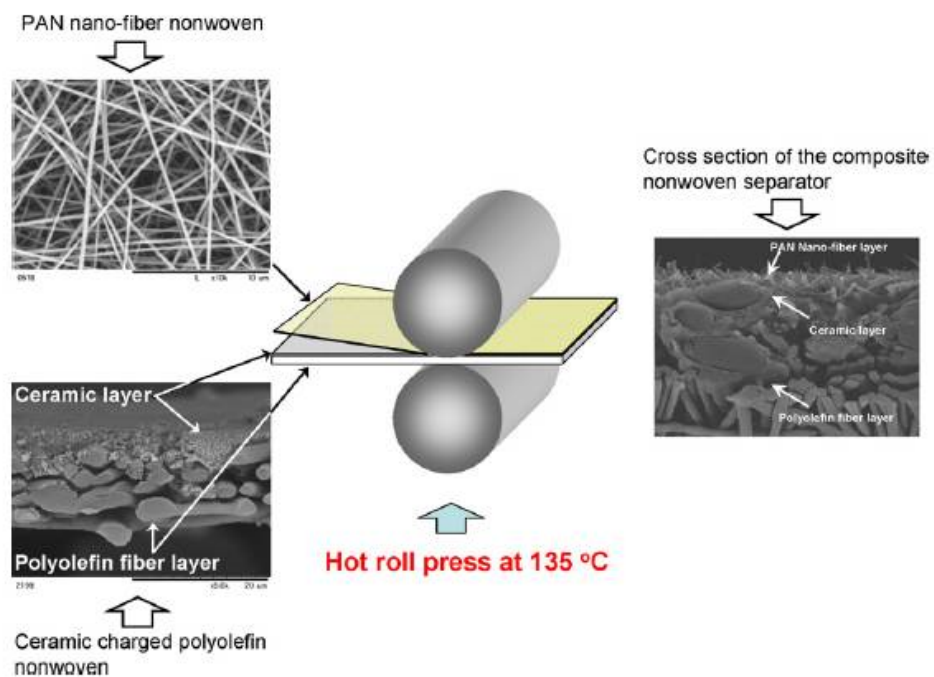


Figure 17. Schematic of laminating process and the morphology of composite membrane [241]. Reproduced with the permission.

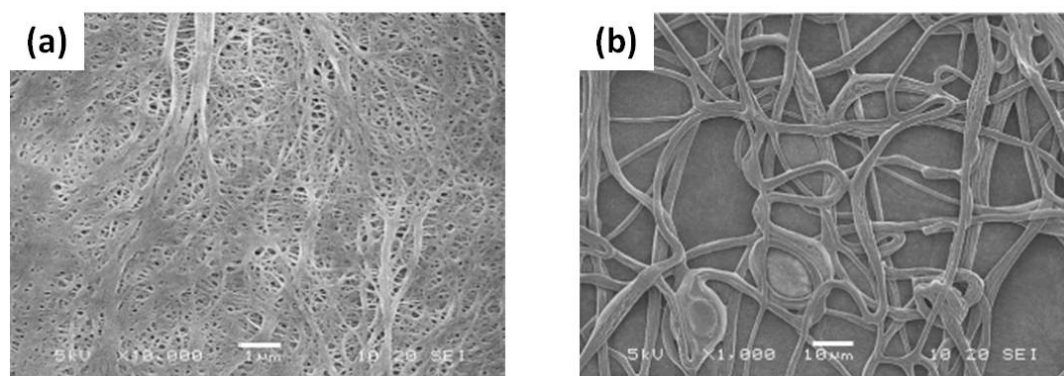


Figure 18. SEM images of (a) PE membrane and (b) $\text{Al}_2\text{O}_3/\text{PVDF-co-CTFE}$ fiber-coated PE membrane [242]. Reproduced with the permission.